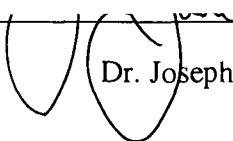


## AN ABSTRACT OF THE THESIS OF

Nilobon Podhipeux for the degree of Master of Science in Food Science & Technology presented on November 18, 1994. Title: Adsorption of Selected Charge Mutants of Bacteriophage T4 Lysozyme at Silanized Silica Surfaces.

Abstract approved: \_\_\_\_\_

  
Dr. Joseph McGuire

The adsorption kinetics exhibited by selected charge mutants of T4 lysozyme at silanized silica surfaces were monitored with *in situ* ellipsometry. Mutant lysozymes were produced by substitution of lysine (Lys) with glutamic acid (Glu). Each substitution resulted in a decrease in the net charge of the protein by 2 units. The wild type lysozyme of net charge +9, and two mutants of net charge +7 and +5 were obtained from *E. coli* strain RR1. Adsorption kinetics recorded at hydrophilic and hydrophobic interfaces were compared to the kinetic behavior predicted by two simple models for protein adsorption. One was a three-rate-constant model allowing for reversible adsorption followed by conversion to an irreversibly adsorbed form, and was analyzed under three different conditions. The first condition allowed the adsorption rate ( $k_1$ ) and the desorption rate ( $k_{-1}$ ) to be variable while the surface-induced conversion rate ( $s_1$ ) was assumed constant. The second condition assumed  $k_1$  and  $k_{-1}$  constant instead of  $s_1$ , and the third allowed all kinetic rate constants to be variable. The second model allowed for irreversible adsorption into one of two states directly from solution. Both models suggested that substitution of Lys with Glu in the backbone of T4 lysozyme facilitates the adsorption of the protein at these interfaces. Proteins apparently adsorbed at the interfaces more tightly and occupied a greater interfacial area with substitution of Lys with Glu, and these effects were related

to the location of the substitutions relative to other charged residues of the protein, and not to net charge.

Adsorption of Selected Charge Mutants  
of Bacteriophage T4 Lysozyme at Silanized Silica Surfaces

by

Nilobon Podhipleux

A THESIS

submitted to

Oregon State University

in partial fulfillment of  
the requirements for the  
degree of

Master of Science

Completed November 18, 1994  
Commencement June, 1995

Master of Science thesis of Nilobon Podhipleux presented on November 18, 1994

APPROVED:

---

Major Professor, representing Food Science & Technology

---

Head of Department of Food Science & Technology

---

Dean of Graduate School

I understand that my thesis will become part of the permanent collection of Oregon State University libraries. My signature below authorizes release of my thesis to any reader upon request.

---

Nilobon Podhipleux, Author

## ACKNOWLEDGEMENT

I wish to express my great gratitude to Dr. Joseph McGuire, my major professor, for his valuable guidance and support. I would like to thank Dr. Edward R. Kolbe, Dr. Ronald E. Wrolstad, and Dr. Peter R. Cheeke for kindly serving as my committee members.

My appreciation is also extended to Dr. Viwat Krisdhasima and my co-worker, Brigesh Singla, for their suggestions, friendship and support. Special thanks to Professor Matthews and Shila Snow of the Institute of Molecular Biology, University of Oregon, for providing bacterial strains needed for this research, as well as Dr. David E. Williams, for allowing me to use facilities in his laboratory.

Without the financial support from the National Science Foundation, the Medical Research Foundation of Oregon, and the Whitaker Foundation, this research would not have been completed.

## TABLE OF CONTENTS

	<u>Page</u>
<b>1. INTRODUCTION</b> .....	1
<b>2. LITERATURE REVIEW</b> .....	3
2.1 Multiple States and Bilayer Adsorptions.....	3
2.2 Effects of pH, Ionic Strength, and Charge.....	6
<b>3. THEORY</b> .....	12
3.1 Basic Features of Protein Adsorption.....	12
3.2 Surface-Induced Conformational Change.....	12
3.3 Adsorption Mechanisms and Kinetic Models.....	13
3.4 Bacteriophage T4 Lysozyme.....	15
<b>4. MATERIALS AND METHODS</b> .....	21
4.1 Lysozyme Production and Purification.....	21
4.2 Preparation of Protein Solution.....	24
4.3 Surface Preparation.....	25
4.4 Adsorption Kinetics.....	25
<b>5. RESULTS AND DISCUSSION</b> .....	27
5.1 Visual Analysis of Kinetic Plots.....	27
5.2 Comparison of Adsorption Kinetics on Hydrophilic and Hydrophobic Silica.....	34
5.3 Comparison to Kinetic Models.....	44
<b>6. CONCLUSION</b> .....	56
<b>BIBLIOGRAPHY</b> .....	57
<b>APPENDICES</b> .....	62

## LIST OF FIGURES

<u>Figure</u>	<u>Page</u>
3.1 Three-rate-constant adsorption mechanism.....	18
3.2 Parallel adsorption mechanism.....	19
3.3 Backbone of phage lysozyme, showing the amino acid substitutions in M135, and M135/145.....	20
5.1 Adsorption kinetics of wild type on hydrophilic silica.....	28
5.2 Adsorption kinetics of M135 on hydrophilic silica.....	29
5.3 Adsorption kinetics of M135/147 on hydrophilic silica.....	30
5.4 Adsorption kinetics of wild type on hydrophobic silica.....	31
5.5 Adsorption kinetics of M135 on hydrophobic silica.....	32
5.6 Adsorption kinetics of M135/147 on hydrophobic silica.....	33
5.7 Adsorption kinetics of wild type on hydrophilic and hydrophobic silica.....	35
5.8 Adsorption kinetics of M135 on hydrophilic and hydrophobic silica.....	36
5.9 Adsorption kinetics of M135/147 on hydrophilic and hydrophobic silica.....	37
5.10 Adsorption kinetics of wild type, M135, and M135/147 on hydrophilic silica.....	38
5.11 Adsorption kinetics of wild type, M135, and M135/147 on hydrophobic silica.....	39
5.12 Possible adsorption behavior of T4 lysozyme on the hydrophilic surface.....	41
5.13 Possible adsorption behavior of T4 lysozyme on the hydrophobic surface....	43
5.14 Comparison plots between model fitting and experimental data.....	52

## LIST OF TABLES

<b><u>Table</u></b>	<b><u>Page</u></b>
5.1 Adsorbed mass after 8 h.....	27
5.2 The distribution of mobile charges for each protein.....	40
5.3 Fraction of adsorbed molecules that were rinsable following 30 min contact with hydrophilic and hydrophobic silica.....	42
5.4 Values of the ratios $k_{-1}/k_1C$ obtained by analysis of kinetic data with Eqs.[5] and [6], holding $s_1$ constant.....	45
5.5 Values of the rate constants $k_1$ , $k_{-1}$ , and $s_1$ obtained by analysis of kinetic data with Eq.[5] and [6], holding $k_1$ and $k_{-1}$ constant.....	47
5.6 Averaged values of $r_1$ and $r_2$ for each protein-surface contact, and the corresponding values of $s_1k_1C$ for each case, calculated according to Eq.[6].....	49
5.7 Averaged values of $k_2/k_1$ obtained by non-linear regression analysis of kinetic data with Eq.[11].....	51
5.8 Averaged values of $k_2/k_1$ obtained by linear regression analysis of kinetic data with Eq.[11].....	54



## LIST OF APPENDICES

<u>Appendix</u>		<u>Page</u>
A	M/A ratios and specific volumes of each protein.....	62
B	Preparation of broths, buffers, and solutions.....	63
C	Averaged values of kinetic rate constants from the three-rate-constant model, assuming $k_1$ and $k_{-1}$ are depending on electrostatic interaction between the protein and the surface.....	65
D	Averaged values of kinetic rate constants from the three-rate-constant model, assuming $k_1$ and $k_{-1}$ are unaffected by protein charges.....	72
E	Values of the kinetic model parameters from the three-rate-constant model.....	77
F	Values of the kinetic model parameters from the parallel adsorption model, using non-linear regression analysis...	79
G	Values of the kinetic model parameters from the parallel adsorption model, using linear regression analysis.....	81
H	Raw Data of all experiments.....	84

## LIST OF APPENDIX TABLES

<u>Table</u>	<u>Page</u>
A.1 M/A ratios and the specific volumes of each protein used in OEP program.....	62
B.1 Preparation of LB broth (overnight) and LB-H broth (fermentation broth).....	63
B.2 Preparation of buffers and solutions.....	64
C.1 Averaged values of $k_1$ , $k_{-1}$ , and the ratio $k_{-1}/k_1C$ of wild type on hydrophilic silica.....	66
C.2 Averaged values of $k_1$ , $k_{-1}$ , and the ratio $k_{-1}/k_1C$ of M135 on hydrophilic silica.....	67
C.3 Averaged values of $k_1$ , $k_{-1}$ , and the ratio $k_{-1}/k_1C$ of M135/147 on hydrophilic silica.....	68
C.4 Averaged values of $k_1$ , $k_{-1}$ , and the ratio $k_{-1}/k_1C$ of wild type on hydrophobic silica.....	69
C.5 Averaged values of $k_1$ , $k_{-1}$ , and the ratio $k_{-1}/k_1C$ of M135 on hydrophobic silica.....	70
C.6 Averaged values of $k_1$ , $k_{-1}$ , and the ratio $k_{-1}/k_1C$ of M135/147 on hydrophobic silica.....	71
D.1 Averaged $s_1$ values for each protein on hydrophilic surfaces.....	73
D.2 Averaged $s_1$ values for each protein on hydrophobic surfaces.....	74
D.3 Averaged values of kinetic rate constants for lysozyme on hydrophilic silica.....	75
D.4 Averaged values of kinetic rate constants for lysozyme on hydrophobic silica.....	76
E.1 Values of the kinetic model parameters from the three-rate-constant model for each protein on hydrophilic surfaces.....	77

**LIST OF APPENDIX TABLES (Continued)**

<b><u>Table</u></b>		<b><u>Page</u></b>
E.2	Values of the kinetic model parameters from the three-rate-constant model for each protein on hydrophobic surfaces.....	78
F.1	Values of the kinetic model parameters from the parallel adsorption model for each protein on hydrophilic surfaces, using non-linear regression analysis.....	79
F.2	Values of the kinetic model parameters from the parallel adsorption model for each protein on hydrophobic surfaces, using non-linear regression analysis.....	80
G.1	Values of the kinetic model parameters from the parallel adsorption model for each protein on hydrophilic surfaces, using linear regression analysis.....	82
G.2	Values of the kinetic model parameters from the parallel adsorption model for each protein on hydrophobic surfaces, using linear regression analysis.....	83

# **ADSORPTION OF SELECTED CHARGE MUTANTS OF BACTERIOPHAGE T4 LYSOZYME AT SILANIZED SILICA SURFACES**

## **CHAPTER 1**

### **INTRODUCTION**

The behavior of proteins at interfaces has been the subject of numerous studies during the last few decades. Most practical systems involving biological fluids contain a mixture of different proteins. When these protein molecules come in contact with an interface, they adsorb spontaneously and interfacial properties are altered as a consequence (Andrade, 1985).

In the food industry, proteins play a major role in the fouling of heat-exchange surfaces and membrane surfaces because of their heat sensitivity and high concentration (Luey et al., 1991). These films can lead to increased resistance both to liquid flow and heat transfer, causing considerable economic losses associated with processing and cleaning (Criado et al., 1994). Since microbial and spore adhesion appear to be mediated by protein adsorption (Tosteson et al., 1975 and Bryers, 1987), health problems related to bacterial contamination, in addition to recall and destruction of food products, may occur as a result of events initiated by protein fouling. The amount of adhered cells and the rate of microbial adhesion to surfaces are dependent on the molecular properties of the pre-adsorbed proteins (Al-Makhlafi et al., 1994).

Recently, preadsorption of bactericidal proteins as a barrier to bacterial adhesion to fluid-milk contact surfaces was reported (Daeschel et al., 1992). Displacement of the preadsorbed proteins by incoming milk serum proteins of higher affinity would be the major problem affecting the long-term stability of such surfaces. Other food-related aspects affected by proteins at interfaces include foam and emulsion formulation and

stability. When milk proteins such as  $\alpha$ -lactalbumin,  $\beta$ -lactoglobulin, and bovine serum albumin accumulate at air-water or oil-water interfaces, the resulting interfacial layer can serve as a foam or emulsion stabilizer by reducing interfacial tension and rates of collapse and coalescence. Many food products are foams, emulsions, or both, and proteins can play an important role in stabilizing these systems. However, molecular factors that influence protein functionality in such system is far from completely understood, and in a real quantitative sense, not understood at all.

It has been difficult to quantitatively study the protein adsorption process since the surface activity of a protein is a cumulative property influenced by its size, shape, charge, thermal stability, and many other factors. Proteins can vary substantially with respect to each of these properties (Suttiprasit et al., 1992). Therefore, until very recently it has been impossible to compare two proteins that differ from each other in only one of these aspects. The use of synthetic protein mutants obtained from site-directed mutagenesis holds promise for gaining a more quantitative understanding of protein behavior at solid surfaces, as chosen molecular properties can be related unambiguously to protein surface activity (Kato et al., 1988, and Horbett, 1988).

The objective of this research was to gain a better understanding of charge influences on adsorption by studying the adsorption of charge mutants of a single protein that insignificantly differ in structural stability and three-dimensional structure. In this research, two charge mutants of bacteriophage T4 lysozyme, along with the wild type protein, were selected to study the effects of protein charge on adsorption to silanized hydrophobic and hydrophilic silica surfaces. A summary of related studies, and principals of protein adsorption as well as basic features of model proteins are provided in the following Chapters.

## CHAPTER 2

### LITERATURE REVIEW

#### 2.1 Multiple States and Bilayer Adsorptions

##### 2.1.1 Multiple States of Adsorption

Although many investigators have frequently applied the Langmuirian monolayer model to protein adsorption isotherms, many researchers believe that protein can adsorb onto a surface in more than one state. Study that supports the multiple states theory involves comparison of adsorption isotherms obtained from single-step and successive addition of protein. Jönsson et al. (1987) studied the adsorption behavior of secretory fibronectin and immunoglobulin G and found differences between isotherms constructed on hydrophobic silica using the single-step and the successive addition methods for each protein. These results indicated virtual irreversibility of the adsorption process due to surface-dependent conformational changes occurring over time. DeFeijter et al. (1978) studied the adsorption of various proteins at air-water interfaces and related adsorption to the availability of adsorption sites at the contact interface. They suggested that the degree to which adsorbed molecules change their conformation depends on the number of adsorbed molecules at the surface. For low bulk concentration conformational rearrangement of the adsorbed molecules is considerable while the adsorbed molecules is hardly affected for high bulk concentrations. These adsorption isotherms and adsorbed kinetics cannot be explained by a simple Langmuir type of adsorption.

After trying several models based on Langmuir-like behavior which could not adequately explain protein adsorption on a solid surface, Lundström (1985) proposed a simple dynamic equilibrium model for protein adsorption. This model allows two forms of adsorbed protein; i.e., a "native" and "denatured" form. Proteins adsorbed in each of these

states cover a different surface area and can desorb into the solution. This equilibrium model accounts for the possibility of protein molecules changing conformation or orientation on solid surfaces.

Later, Lundström and Elwing (1990) proposed a more complicated protein adsorption model. In this model, several forms of adsorbed molecules are allowed, and adsorbed molecules can be exchanged with molecules from the bulk solution. In each case however, the rate constants cannot be estimated because of the model complexity, and this model is not very helpful in the interpretation of experimental data.

Based on the model suggested by Lundström (1985), Krisdhasima et al. (1992b) studied the adsorption kinetics of  $\beta$ -lactoglobulin and recommended a modified model that is less complicated, i.e., governed by fewer rate constants. In this study, they used 5 different concentration of dichlorodimethylsilane (DDS) in xylene (0.01, 0.025, 0.05, 0.1, and 1 %) to silanize silica surfaces. A protein concentration of 1 mg/mL was selected as it was a relatively low value that would still minimize diffusional limitations. They found that the pattern of the kinetic data at each surface agreed well with the model. In their model, protein adsorption is divided into two steps. In step 1, protein molecules reversibly adsorb onto the surface. In step 2, corresponding to long contact time, adsorbed protein molecules undergo surface-induced conformational transformation to an irreversibly adsorbed form. It might not be appropriate to assume that generation of irreversibly adsorbed molecules can occur only through the conformational change of reversibly adsorbed molecules. Moreover, it should be taken into account that molecules in both states are assumed in this model to cover the same surface area.

McGuire et al. (1994c) studied the comparative adsorption of synthetic mutants of bacteriophage T4 lysozyme, using 4 charge mutants, 3 stability mutants, and wild type. Their data indicated that a molecule in a more tightly bound state occupied a greater interfacial area than that in a less tightly bound state. Their data also indicated that attainment of the more tightly bound state was faster than what would have been

consistent with the kinetic model proposed by Krisdhasima et al. (1992b). They suggested a model in which protein molecules can adopt one of two states directly from bulk solution. State 1 molecules, compared with those in state 2, occupy less specific area, and are less tightly bound, as verified by their elutability by a solution of 0.03M DTAB (dodecyltrimethylammonium bromide).

Strong evidence supporting the presence of multiple states of adsorbed protein comes from elutability studies. Bohnert and Horbett (1986) studied the ability of sodium dodecylsulfate (SDS) to remove fibrinogen and albumin from the surface of polymers. They found that the elutability of both proteins decreased as the contact time increased. This suggested that the binding strength of adsorbed molecules had increased over time. When further attempts were made to remove proteins with various detergents, they found that more proteins were removed but elution was incomplete.

More recently, Krisdhasima et al. (1993) studied adsorption kinetics and elutability of  $\alpha$ -lactalbumin,  $\beta$ -casein,  $\beta$ -lactoglobulin, and bovine serum albumin. They found that after being rinsed with the same buffer used for adsorption for 15 minutes (flow rate 10 mL/min), followed by contact with that buffer for 30 minutes; some protein molecules were removed. More molecules were removed after being incubated in SDS (3% wt/vol.) for 30 minutes, however, not all molecules on the surface were eluted. This supports the thought that protein molecules can adsorb in multiple states, ranging from being weakly to more tightly bound.

### 2.1.2 Bilayer Adsorption

Many researchers have reported that proteins can adsorb onto a surface in more than one layer; among these are Walton and Maenpa (1979), Arnebrant et al. (1985), and Arnebrant and Nylander (1988). Walton and Maenpa (1979) used fluorescence spectroscopy as a means to study the adsorption behavior of bovine serum albumin on



copolyptide particles. They found that the change in fluorescence is due to adsorbed protein molecules and loosely bound molecules in close proximity to the first layer.

Arnebrant et al. (1985) studied the adsorption behavior of  $\beta$ -lactoglobulin and ovalbumin on hydrophobic and hydrophilic chromium oxide surfaces. Ellipsometry and electrical potential measurements were used. Ellipsometric data showed that a thick, highly hydrated layer, which can be partially removed by rinsing, was formed on hydrophilic surfaces. The results suggested that proteins adopted a bilayer formation with a loosely bound layer on the top, and a tightly bound layer at the bottom. This bottom layer was strongly attached to the surface and not removable by rinsing. Arnebrant and Nylander (1988) also reported the possibility of bilayer formation by insulin, caused by protein polymerization. In the studies done by McGuire et al. (1994a, b, c), data suggested that T4 lysozyme formed a second layer which was removable by rinsing with buffer.

## **2.2 Effects of pH, Ionic Strength, and Charge**

In protein adsorption studies, sorbent properties such as charge density and hydrophobicity as well as environmental conditions such as pH and ionic strength are often taken as experimental variables. It is because the three-dimensional structure of a protein is the result of various interactions (hydrophobic interaction, hydrogen bonding, electrostatic interactions, S-S bonds, etc.) inside the protein molecule as well as between the protein and its environment (Arai and Norde, 1990a). Since proteins are such complicated molecules, it is difficult to control its intrinsic properties, and environmental conditions are normally chosen as variables in the study of electrostatic effects on protein adsorption.

### 2.2.1 pH Effects

The net charge of a protein in solution is dependent on the difference between pH of the solution and the isoelectric point of that protein. If pH of the solution is greater than the isoelectric point of the protein, the net charge of the protein is negative. If pH of the solution is less than the isoelectric point of the protein, the net charge of the protein in that solution is positive. Many researches showed that maximum adsorption generally occurs near the isoelectric point. When the net charge of a protein is greater, it will be in a more extended form whereas a protein will be in a more globular form if its net charge is smaller. Since a globular molecule requires less area for adsorption when compared with the extended form, it is likely that the adsorption of a more globular molecule is greater (Lee and Ruckenstein, 1988).

Norde and Lyklema (1978a) suggested that the degree to which pH affects the adsorption of a protein is determined by its conformational stability. They observed that plateau values of adsorbed protein were independent of pH for bovine pancreas ribonuclease (RNase), whereas those of human plasma albumin (HPA) varied by as much as a factor of two. HPA exhibited a higher degree of conformational adaptability when compared with RNase. This allowed HPA to change its structure as the conditions in the solution changed. The change in its structure was observed in term of adsorbed mass as a function of pH. Unlike HPA, the lack of change in the RNase structure as the pH of the solution changed was reflected in the unaffected adsorbed mass.

The effect of pH on adsorption and desorption of protein was studied by Bagchi and Birnbaum (1981), using goat and rabbit immunoglobulin G. They found that changing the pH of solution from 4.0 to 7.8 and from 10.0 to 7.8 did not cause the adsorbed mass to reach the same amount obtained at pH 7.8.

Kondo and Higashitani (1992) studied the adsorption of model proteins with wide variation in molecular properties. They explained the pH dependence of the plateau

adsorption of large proteins in term of lateral interaction. They suggested that the lateral interaction between larger protein molecules is stronger than that of smaller molecule. Therefore, the larger proteins showed maximum adsorption around their isoelectric points, at which their net charge was zero, whereas the trend was less pronounced for the smaller proteins due to the smaller effect of lateral interactions. Since lateral interactions between adsorbed proteins was reduced by electrolyte, the pH dependence of plateau adsorption were mainly determined by the nature of the dominant interaction between proteins and surfaces, e.g., the electrostatic interaction is dominant in the interaction between a protein and a hydrophilic surface, thus, the plateau adsorption at a negatively charged surface showed a significant decrease with increasing pH.

### 2.2.2 Ionic Strength Effects

The degree to which ionic strength affects protein adsorption is a function of the role electrostatics plays in the adsorption driving force. At low ionic strength surface charges of proteins fully contribute to the total electrostatic interaction (Lee and Ruckenstein, 1988). At higher ionic strength, the surface charges of proteins are shielded. This results in reduced interactions between protein molecules (Baghi and Birnbaum, 1981); as a consequence, a greater amount of protein is expected to adsorb. Previous work has shown a general trend of an increase in the amount of protein adsorbed as ionic strength increases (Jönsson et al., 1987; Soderquist and Walton, 1980). Luey et al. (1991) suggested that the ionic strength influences on adsorbed mass may be related to either protein stability or the surface properties. They observed that increased ionic strength (NaCl concentration) shielded the electrostatic repulsion between the negatively charged protein molecules and a hydrophilic negatively charged surface. Therefore, the adsorbed mass increased as the concentration of NaCl increased. Unlike the hydrophilic surface, the

adsorbed mass on the hydrophobic surface decreased as the concentration of NaCl increased.

### 2.2.3 Charge Effects

Arai and Norde (1990a) studied the adsorption of four proteins of similar molecular mass and shape. They were ribonuclease A (RNase) from bovine pancreas, lysozyme (LSZ) from hen's egg, myoglobin (MGB) from sperm whale, and  $\alpha$ -lactalbumin ( $\alpha$ -LA) from bovine milk. At a given pH, different electrokinetic charge densities are attained because these proteins have different isoelectric points. The results showed that the adsorption of LSZ and RNase on a hydrophilic hematite surface was dominated by electrostatic interaction. On the surface of hydrophobic polystyrene (PS), all proteins adsorbed with high affinities, even under conditions of electrostatic repulsion. However, the electrostatic interaction between the sorbent and proteins was reflected in their plateau values. On the surface of polyoxymethylene (POM), which was slightly negative and less hydrophobic than PS, the electrostatic interactions between the POM crystals and the proteins were relatively weak. The most positively charged protein, LSZ, adsorbed to some extent but the less positive RNase did not, whereas MGB and  $\alpha$ -LA adsorbed at the POM surface although it was not electrostatically favorable. Arai and Norde (1990a) concluded that the adsorption of a globular protein from solution onto a solid surface is related to the stability of its native structure. "Hard" proteins like LSZ and RNase have a large structural stability and a strong internal coherence. Their interaction with an interface is governed by hydrophobic and electrostatic effects. MGB and  $\alpha$ -LA have a relatively low structural stability and possess an additional internal factor that promotes adsorption. This factor is probably related to structural rearrangements involving an increase in conformational entropy. As a consequence, these "soft" proteins may adsorb on a hydrophilic surface under conditions of electrostatic repulsion.

Arai and Norde (1990b) also studied sequential and competitive adsorption, using the same four proteins and three surfaces as mentioned above. They found that in the combinations containing LSZ, RNase, and MGB, sequential and competitive adsorption were largely governed by electrostatic interactions. In the combinations containing  $\alpha$ -LA, however, large sequential adsorption of this protein occurred at all surfaces precoated with another protein, even under electrostatic repulsion. The extraordinary adsorption behavior of  $\alpha$ -LA was possibly related to the weak internal coherence of its globular structure. Arai and Norde suggested that protein structural stability is an important factor that dominates in competitive adsorption, resulting in preferential adsorption of the “soft” proteins over the “hard” ones.

Shirahama et al. (1990) studied comparative protein adsorption. Their results were in line with Arai and Norde (1990a, b). They concluded with three trends supporting that adsorption is determined by electrostatic interaction at hydrophilic surfaces. The first trend they observed was the amount adsorbed from single protein solutions increased with increasing charge contrast between the protein and sorbent surface. Second, sequential adsorption occurred only if the second protein had a more favorable electrostatic interaction with the sorbent surface. Third, the protein having the most favorable electrostatic interaction with the adsorbent preferentially adsorbed from a protein mixture. In the case of hydrophobic surfaces, it was noticed that electrostatic interactions had some effect but did not dominate the adsorption process. It was hypothesized that the adsorption of some proteins on hydrophobic surfaces may be promoted by rearrangement in their molecular structures.

Recently, Elgersma et al. (1992) monitored the adsorption competition between bovine serum albumin (BSA) and immuno-gamma-globulins (IgGs). In this research, electrostatic interactions were systematically examined by using IgGs of different isoelectric points, positively and negatively charged lattices, and by performing experiments at various pH values. Under electrostatically repulsive conditions, the

adsorption competition was found to be strongly influenced by the electrostatic interaction between the surface and the respective proteins. Nevertheless, when the proteins were electrostatically attracted to the surface, the influence of electrostatics on preferential adsorption was hardly discernible.

## **CHAPTER 3**

### **THEORY**

#### **3.1 Basic Features of Protein Adsorption**

Considering the adsorption of a single protein, there are three basic components that affect the protein adsorption process; the nature of the protein, the nature of the medium, and the nature of the solid surface (Andrade, 1985).

The protein properties that generally affect its adsorption are size, shape, charge, thermal stability, isoelectric point, and three-dimensional structure in solution. Solution conditions such as pH, ionic strength, temperature, and hydrodynamics also influence the adsorption, and surface properties have to be taken in to account as well.

Soderquist and Walton (1980) characterized protein adsorption as a time-dependent process, which can be divided into 3 stages:

- (1) at short time, the adsorption is reversible, and no conformational change occurs;
- (2) at longer time, conformational changes occur, and the adsorption is semi-reversible; and
- (3) after a long time, conformational changes are completed, and the adsorption is irreversible.

#### **3.2 Surface-Induced Conformational Change**

It is believed that conformational changes occur during protein adsorption in order to minimize interfacial free energy. When protein molecules in their "native" form adsorb at an interface, they are believed to be induced to adopt a more "spread" form that can bind more tightly to the surface. For example, Andrade et al. (1984) used intrinsic

ultraviolet total internal reflection fluorescence spectroscopy to monitor conformational changes of human plasma fibronectin (HPF) on silica surfaces. Their results indicated that the adsorbed HPF had undergone some conformational changes.

DeFeijter et al. (1978) suggested the extent to which adsorbed molecules change their conformation relates to the availability of adsorption sites on the contact surface, and depends on the number of molecules adsorbed at the surface. Studies also showed that the degree of "denaturation" was directly related to contact time with the surface (Walton and Maenpa, 1979; Soderquist and Walton, 1980).

### 3.3 Adsorption Mechanisms and Kinetic Models

Lundström (1985) developed a model for reversible protein adsorption, based on the hypothesis that molecules go through conformational transformation. According to this mechanism, protein can adsorb in both "native" and "denatured" states.

Krisdhasima et al. (1992b) proposed a very similar mechanism, consisting of two steps, as shown in Figure 3.1. In the first step, a protein molecule reversibly adsorbs, governed by rate constants  $k_1$  and  $k_{-1}$ . In the second step, it undergoes a surface-induced conformational change, governed by rate constant  $s_1$ , to an irreversibly adsorbed form.

Differential equations describing the time-dependent fractional surface coverages of protein in states 1 ( $\theta_1$ ) and 2 ( $\theta_2$ ) are:

$$d\theta_1/dt = k_1C(1 - \theta_1 - \theta_2) - (k_{-1} + s_1)\theta_1 \quad [1]$$

$$\text{and } d\theta_2/dt = s_1\theta_1. \quad [2]$$

The total surface coverage,  $\theta$ , at any time is  $\theta_1 + \theta_2$ , and  $C$  is protein concentration near the interface.

Solving equations (1) and (2) yielded an expression for the total surface coverage as a function of time:

$$\theta = A_1\exp(-r_1t) + A_2\exp(-r_2t) + A_3 \quad [3]$$



where  $A_1$ ,  $A_2$ , and  $A_3$  are constants and roots  $r_1$  and  $r_2$  are known functions of the rate constants  $k_1$ ,  $k_{-1}$ , and  $s_1$ . An expression for total adsorbed mass ( $\Gamma$ ) as a function of time obtained from equation (3) is:

$$\Gamma = a_1 \exp(-r_1 t) + a_2 \exp(-r_2 t) + a_3 \quad [4]$$

where  $a_1$ ,  $a_2$ , and  $a_3$  are the products of the equilibrium adsorbed mass ( $\Gamma_{\max}$ ) with  $A_1$ ,  $A_2$ , and  $A_3$ , respectively.

Non-linear regression analysis performed on adsorption kinetic data allows parameters  $a_1$ ,  $a_2$ ,  $a_3$ ,  $r_1$ , and  $r_2$  to be estimated. The roots are related to the rate constants as follows (Krisdhasima et al., 1992b):

$$r_1 + r_2 = k_1 C + k_{-1} + s_1 \quad [5]$$

and  $r_1 r_2 = s_1 k_1 C. \quad [6]$

In development of this model, it was assumed that generation of irreversibly adsorbed molecules can occur only by the surface-induced conformational transformation after adsorption in the reversible form, and there is no difference in the interfacial area occupied by molecules in states 1 and 2.

McGuire et al. (1994c) studied the comparative adsorption of synthetic mutants of bacteriophage T4 lysozyme. They found that adsorbed molecules in different states occupied different interfacial areas. A more suitable mechanism for adsorption of T4 lysozyme monomers was suggested as is shown in Figure 3.2.

In this case, protein may adopt one of two states, where a state 1 molecule is less tightly bound than one in state 2, and occupies a smaller interfacial area ( $A_1$ ) than it does in state 2 ( $A_2$ ). McGuire et al. (1994c) defined fractional surface coverage  $\theta_1$  as the mass of state 1 molecules adsorbed at any time divided by the maximum mass of molecules that could be adsorbed in a monolayer,  $\Gamma_{\max}$ , and  $\theta_2$  as the mass of state 2 molecules adsorbed at any time divided by  $\Gamma_{\max}$ . In the absence of spontaneous desorption and at monolayer coverage,

$$\theta_1 + a\theta_2 = 1 \quad [7]$$

where  $a$  is  $A_2/A_1$ , and

$$\Gamma = \Gamma_{\max} (\theta_1 + \theta_2). \quad [8]$$

Solving the  $d\theta/dt$  equations:

$$d\theta_1/dt = k_1 C (1 - \theta_1 - a\theta_2)$$

$$d\theta_2/dt = k_2 C (1 - \theta_1 - a\theta_2)$$

yields

$$\theta_1 + \theta_2 = \alpha [1 - \exp(-k_1 C - ak_2 C)t] \quad [9]$$

where  $\alpha$  is a constant. At  $t = 0$ ,  $\theta_1 + \theta_2 = 0$  and as  $t \rightarrow \infty$ ,  $\theta_1 + \theta_2 = \alpha$ .

Knowing that  $k_2/k_1 = \theta_2/\theta_1$  as  $t \rightarrow \infty$ , we can solve for  $\theta_1 + \theta_2$  as a function of  $k_1$  and  $k_2$ :

$$\theta_1 + \theta_2 = \frac{(1 + k_2/k_1)}{1 + ak_2/k_1} \quad [10]$$

therefore

$$\Gamma = \Gamma_{\max} \cdot \frac{(1 + k_2/k_1)}{1 + ak_2/k_1} \cdot [1 - \exp(-k_1 C - ak_2 C)t] \quad [11]$$

Using non-linear regression,  $k_1$  and  $k_2$  can be calculated. Alternatively, linear regression analysis can also be applied to adsorption kinetics plotted on semi-log coordinates to estimate the values of these rate constants.

### 3.4 Bacteriophage T4 Lysozyme

Lysozyme is a hydrolytic enzyme, which cleaves a glycosidic bond in a complex sugar. It destroys bacterial cell walls by hydrolyzing the  $\beta(1 \rightarrow 4)$  glycosidic linkages from N-acetylmuramic acid (NAM) to N-acetylglucosamine (NAG) in the alternating NAM-NAG hexasaccharide component of cell wall peptidoglycans (Grütter and Matthews, 1982). Variants of this enzyme are found in egg-white, tear fluid, and other biological secretions (Zubay, 1983). Phage lysozyme cleaves the same glycosidic bond as

does hen egg-white lysozyme (HEWL), but is 250-fold more active toward *Escherichia coli* cell walls, leading to cell lysis (Grütter et al., 1983).

The structure of lysozyme from bacteriophage T4 was initially determined at 2.4 Å resolution (Matthews and Remington, 1974; Remington et al., 1978) and has been confirmed by high-resolution refinement recently (Weaver and Matthews, 1987). Phage lysozyme has a bilobal structure with the active site located at the junction of 2 domains: the C-terminal and N-terminal lobes. These 2 lobes are joined by an  $\alpha$ -helix (residue 60-80) that traverses the length of the molecule (Alber and Matthews, 1987). The molecule of bacteriophage T4 lysozyme is comprised of 164 amino acid residues with a molecular weight of about 18,700 daltons (Matthews et al., 1973). There are no disulfide linkages present in the molecule (Weaver and Matthews, 1987).

T4 lysozyme is a basic, globular protein molecule with an isoelectric point above 9. The wild type molecule has 27 positively-charged side chains and 18 negatively-charged side chains, yielding an excess of 9 positive charges at neutral pH. Almost all of the out-of-balance charges are located on the C-terminal lobe (Alber and Matthews, 1987; Weaver and Matthews, 1987). Molecular dimensions of T4 lysozyme in solution are ellipsoidal; it is about 54 Å long, with the diameters of the C-terminal and N-terminal lobes being about 24 Å and 28 Å respectively (Grütter and Matthews, 1982; Matthews et al., 1973; Matsumura and Matthews, 1989).

### Charge Mutants

Beside the wild type lysozyme, 2 charge mutants were chosen for study, each involving substitution of a lysine with a glutamic acid residue (Lys  $\rightarrow$  Glu). Glutamic acid was chosen as the replacement residue for two reasons (Dao-pin et al., 1992). First, the choice of this negatively-charged amino acid maximizes the difference in charge per replacement. Second, the hydrocarbon part of the glutamate side-chain resembles that of

lysine, therefore possible changes in hydrophobic packing were minimized. The substitutions were individually and collectively made on the C-terminal lobe (Figure 3.3), yielding the single-point mutant with 7 positive charges (Lys135 → Glu), and the double-point mutant with 5 positive charges (Lys135 → Glu and Lys147 → Glu). These mutants will be abbreviated M135 and M135/147, respectively.

Difference electron density maps (Grütter et al., 1979), crystallographic refinement (Grütter et al., 1983), and high-resolution X-ray analysis (Dao-pin et al., 1992) showed that the differences between the wild type enzyme and the mutant enzymes are subtle. With reference to their catalytic activity, both M135 and M135/147 are fully functional lysozymes (Dao-pin et al., 1992).

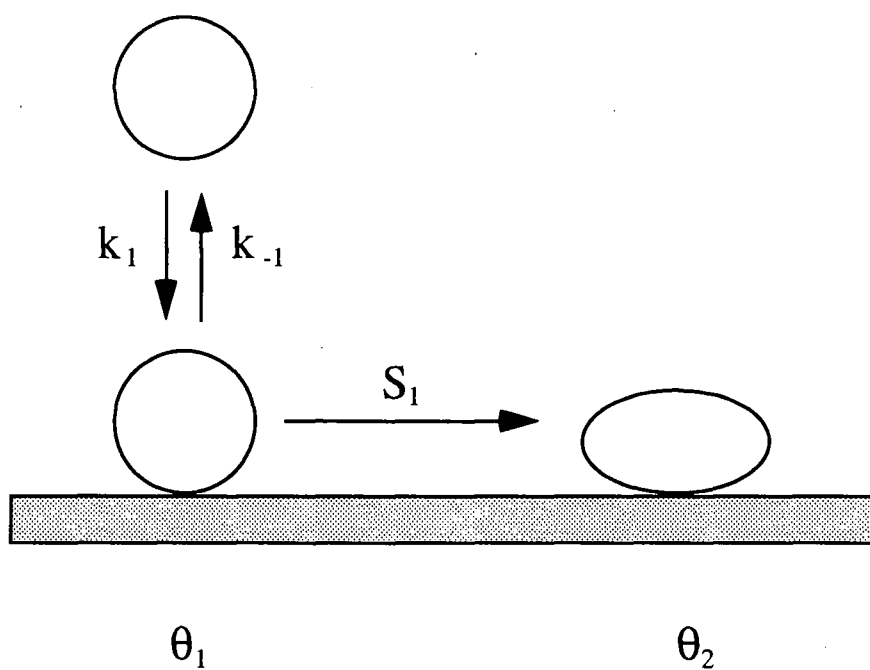


**Figure 3.1.** Three-rate-constant adsorption mechanism (Krisdhasima et al., 1992b).

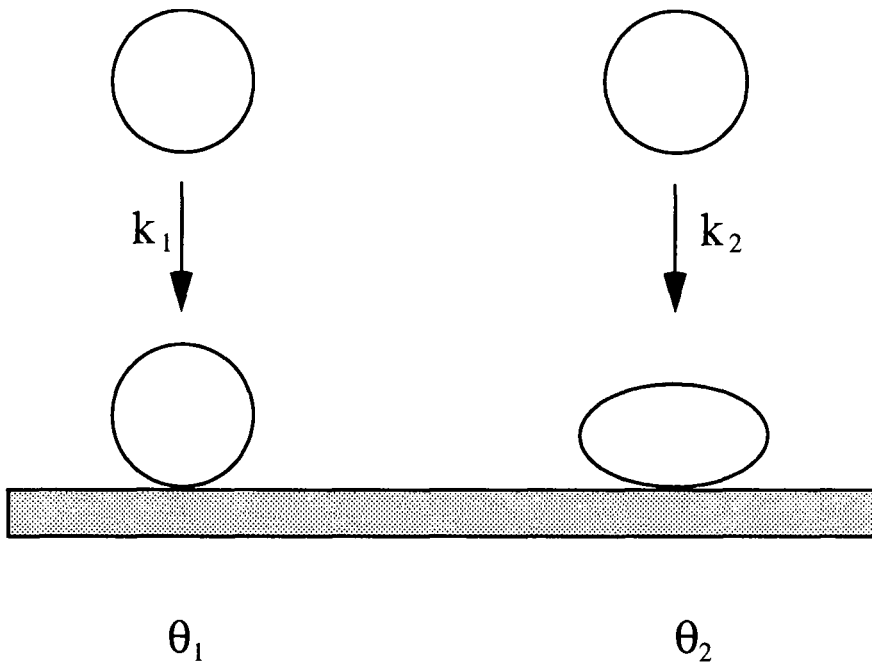


**Figure 3.2.** Parallel adsorption mechanism (McGuire et al., 1994b).

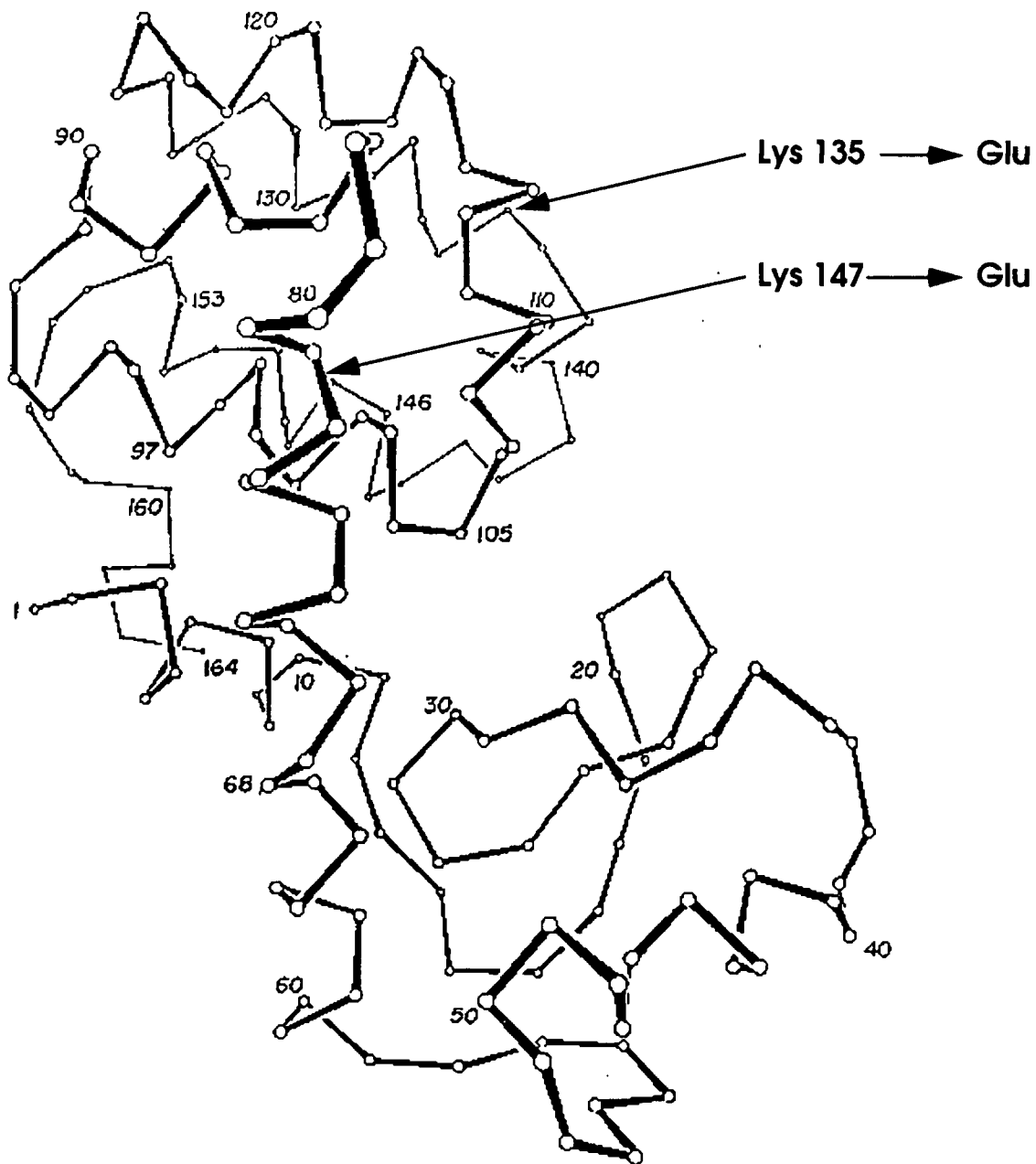


**Figure 3.3.** Backbone of phage lysozyme, showing the amino acid substitutions in M135, and M135/147.

## CHAPTER 4

### MATERIALS AND METHODS

#### 4.1 Lysozyme Production and Purification

Synthetic mutants of T4 lysozyme were produced from transformed cultures of *E. coli* strain RR1, received from Professor Brian Matthews of the Institute of Molecular Biology, University of Oregon. For mutant 135, with a net charge of +7, lysine at position 135 was replaced with glutamic acid. In the case of mutant 135/147, with a net charge of +5, lysine residues at positions 135 and 147 were each replaced with glutamic acid.

##### 4.1.1 Fermentation

Two bottles of overnight broth (1 g tryptone, 0.5 g yeast extract, 0.5 g NaCl, 0.1 mL 1 N NaOH, and 100 mL deionized distilled water (DDW)) were prepared. After autoclaving and cooling down to the room temperature, one loop of glycerol stock culture (-80 °C) was inoculated into each bottle and incubated at 37 °C for approximately 8 h. The overnight cultures were then transferred into an autoclaved fermenter, containing about 4.8 L of sterilized LB broth (57.6 g tryptone, 24 g yeast extract, 48 g NaCl, 4.8 g glucose, and 4.8 L DDW) Tributyl phosphate (Sigma Chemical Co., St. Louis, MO) 1.5 mL was added as an anti-foaming agent together with 0.4 g of ampicillin to prevent contaminant growth. Fermentation was held at 37 °C by using a water bath with a circulating system (Model 1120, VWR Scientific, Portland, OR). Agitation was maintained at 600 rpm with a speed controller (ADI 1012, Applikon Dependable Instruments, Schiedam, Holland) while the air flow rate was fixed at "150" on the flow rate meter (Cole-Parmer Instrument Co., Chicago, IL).



When the optical density (OD) of the fermented fluid at 595 nm (DU 62 Spectrophotometer, Beckman Instruments, Inc., Fullerton, CA) was between 0.9 and 1.0, the temperature was decreased to 30<sup>o</sup> C. Isopropyl- $\beta$ -D thiogalactopyranoside (IPTG; 0.75 g dissolved in 10 mL DDW; Sigma Chemical Co., St. Louis, MO) was added to the fermenter in order to initiate cell lysis. Air flow rate was adjusted to "65", and the agitation rate was lowered to 200 rpm. Harvesting was done 1 hour and 45 minutes after adding IPTG, by siphoning the fluid into 250 mL plastic bottles (DuPont Medical Products, Hoffman Estate, IL).

#### 4.1.2 Centrifugation

Harvested fluid was centrifuged at 4<sup>o</sup>C, 12k rpm (F16/250 Sorvall RC28S, DuPont Medical Products, Hoffman Estate, IL) for 20 minutes. Supernatant was re-centrifuged at 12.5k rpm for 30 minutes, and the second-spin pellet was discarded. The first-spin pellet was resuspended in resuspension buffer ( 10 mM Tris, pH 7.4) and lysis buffer (0.1 M phosphate, 0.2 M NaCl, 10 mM MgCl<sub>2</sub>). The solution of 0.5 M ethylenediamine tetraacetic acid (EDTA, Sigma Chemical Co.) was added to the resuspended solution (1 mL of EDTA solution for every 100 mL of resuspended solution). The solution was then stirred in the cold room (maintained at 4<sup>o</sup>C) for about 12 hours. 1 mL of 1 M MgCl<sub>2</sub> was then added to every 100 mL of resuspended solution. Then 0.01 g of deoxyribonuclease I (DNase I; crude powder from bovine pancreas, Sigma Chemical Co.) was added and the solution was stirred at room temperature for 2 hours. After that, it was centrifuge at 4<sup>o</sup> C and 20k rpm (F28/50 Sorvall RC28S, DuPont Medical Products) for 30 minutes. The pellet was discarded, and the supernatant was combined with the supernatant from the previous spin in 1200 mL fleakers.

#### 4.1.3 Protein Purification

Spectrum dialysis was done against DDW, using Spectra/Por regenerated cellulose (RC) hollow fiber bundles (MWCO 18,000, Spectrum Medical Industries, Inc., Houston, Texas) until the conductivity of the fluid dropped to 2  $\mu\text{ohm/cm}$ , and the pH was between 6.5 and 7.5 (adjust with 1 N NaOH or 1 N HCl if needed). This process required 36 to 48 hours.

Dialyzed supernatant was loaded into a Sepharose column (CM Sepharose CL-6B CCL-100, Sigma Chemical Co.) after the column was packed and settled with 1 L of 50 mM Tris buffer, pH 7.4 (normally requiring about 1 h). After loading the column (requiring about 2 days), a thick, white band of protein would be observed on the Sepharose column which was yellow.

The Sepharose column was rinsed with 150 to 200 mL of 50 mM Tris buffer until the column turned from yellow to white. A salt gradient of 50 mM to 0.3 M NaCl in 50 mM Tris buffer was used to elute the column into a fraction collector (Frac-100, Pharmacia LKB Biotechnology, Alameda, CA). The eluent was monitored with a UV monitor (Optical unit UV-1 and Control unit UV-1, Pharmacia LKB Biotechnology), and output was recorded by a chart recorder.

Fractions that contained protein were combined in Spectra/Por molecularporous membrane tubing (MWCO 12-14K, Spectrum Medical Industries, Inc.), and were dialyzed against phosphate buffer (20 folds the eluent volume), pH 5.8 for about 12 hours. The OD at 280 nm was measured before loading the protein solution onto a Sephadex column for concentration.

#### 4.1.4 Concentration

Protein solution was then loaded onto a Sephadex column (SP Sephadex C50, Sigma Chemical Co.). To elute the concentrated protein, phosphate buffer, pH 6.5, was added to the column drop by drop. Concentrated protein was kept in 2 mL vials in the cold room until use.

The concentrated protein was diluted 1:100 with phosphate buffer, pH 6.5, and its OD at 280 nm was measured to determine the amount of pure protein obtained. To calculate the amount of protein obtained, OD was divided by 1.28.

Sodium dodecylsulfate polyacrylamide electrophoresis (SDS-PAGE) was used to check the purity of protein and only one protein band was observed for each run.

#### **4.2 Preparation of Protein Solution**

Lysozyme from the stock solutions was diluted with phosphate buffer, pH 7 to obtain a protein concentration equivalent to 1 mg/mL of  $\beta$ -lactoglobulin. Buffer solution was prepared by titration of 0.01 M sodium phosphate monobasic monohydrate ( $\text{NaH}_2\text{PO}_4 \cdot \text{H}_2\text{O}$ ) and 0.01 M sodium phosphate dibasic ( $\text{NaH}_2\text{PO}_4$ ). The solution of 0.02% (mass/volume) of sodium azide ( $\text{NaN}_3$ ) was also added as an anti-microbial agent. Protein and buffer solutions were filtered (0.22 mm type GV, Millipore Corp., Bedford, MA).

### 4.3 Surface Preparation

Preparation of hydrophilic and hydrophobic surfaces was done according to similar methods described by Krisdhasima et al. (1992b, 1993) and Suttiprasit and McGuire (1992). The only difference was that in this research surfaces were silanized with dichlorodiethylsilane (DDES) instead of dichlorodimethylsilane.

Silicon (Si) wafers (hyperpure, type N, phosphorous doped, plane 1-0-0) were purchased from Wacker Siltronic Corporation (Portland, OR). By using a tungsten pen, they were cut into approximately 1x2 cm plates. Each of them was placed into a test tube, and 5 mL of 1:1:5 of  $\text{NH}_4\text{OH}:\text{H}_2\text{O}_2:\text{H}_2\text{O}$  was added. Then, they were heated to 80 °C in a water bath for 15 minutes. After rinsing with 20 mL DDW (Corning Mega Pure System, Corning, NY), 5 mL of 1:1:5 of  $\text{HCl}:\text{H}_2\text{O}_2:\text{H}_2\text{O}$  was added. After heating to 80 °C for 15 minutes, they were rinsed with 30 mL DDW, and stored in 50% ethanol in order to maintain stability in hydrophilicity.

Si plates were then rinsed with 40 mL DDW, dried with  $\text{N}_2$ , and kept in a desiccator for 24 h to make sure that the surfaces were water-free. Then they were treated to be hydrophobic by immersion in a solution of dichlorodiethylsilane (DDES, Aldrich Chemical Co., Inc., Milwaukee, WI) in xylene for 1 h. In this research, 0.01% and 0.1% DDES were used for hydrophilic and hydrophobic surfaces, respectively.

Finally, the silanized surfaces were rinsed in 100 mL xylene, acetone, and ethanol. Hydrophobic and hydrophilic surfaces were then blown dry with  $\text{N}_2$ , and kept in desiccators until used.

### 4.4 Adsorption Kinetics

A bare surface, either hydrophobic or hydrophilic, was placed into a fused-quartz, trapezoid cuvette (Hellma Cells, Germany), which was placed on the sample stage of an

automatic ellipsometer (Model L116C, Gaertner Scientific Corp., Chicago, IL). The ellipsometer stage was adjusted to obtain a maximum in reflected light intensity ( $70^{\circ}$  angle of incidence, 1mW Helium-neon laser, wavelength 6328 Å). 6.5 mL of phosphate buffer, pH 7, was injected into the cuvette. Fine adjustments of the sample stage were done to yield steady values of  $\Psi$  and  $\Delta$  (Krisdhasima et al., 1992b; Suttiprasit and McGuire, 1992)..  $\Psi$  is the arctangent of the factor by which the amplitude ratio change, and  $\Delta$  is the steady value of changes in phase of light. Final measurements of bare surface properties, determined by computer software ("SubCA", Gaertner Scientific Corp.) were recorded onto a diskette. Buffer solution was then replaced with 6.5 mL of protein solution. The values of  $\Psi$  and  $\Delta$  were measured ellipsometrically and recorded onto a diskette every 30 s for 8 h. Similar methods were used by Krisdhasima et al. (1992b, 1993).

A one-film-model ellipsometry program (Krisdhasima et al., 1992a) was used to determine refractive index, thickness, and the adsorbed mass of each protein film on each surface.

Experiments with each protein on each type of surface were replicated at least three times to decrease experimental error associated with the results.

## CHAPTER 5

### RESULTS AND DISCUSSION

#### 5.1 Visual Analysis of Kinetic Plots

Some representative plots of the adsorption kinetics exhibited by the proteins are shown in Figures 5.1 to 5.6. The final adsorbed mass after 8h of each protein on each type of surfaces was individually estimated from the kinetic plots of each run by visual inspection. The averaged value of adsorbed mass after 8h was then calculated for each protein on each type of surfaces and is shown in Table 5.1. According to the data shown in Table 5.1 the plateau value attained by wild type is the highest on hydrophilic surfaces, followed by those of M135 and M135/147, respectively. At hydrophobic surfaces, the final adsorbed mass decreases in the order of wild type, M135/147, and M135.

**Table 5.1.** Adsorbed Mass after 8h.

Protein	Adsorbed Mass ( $\mu\text{g}/\text{cm}^2$ )
Wild Type (+9)	
- Hydrophilic	$0.258 \pm 0.029$
- Hydrophobic	$0.225 \pm 0.014$
M135 (+7)	
- Hydrophilic	$0.253 \pm 0.026$
- Hydrophobic	$0.213 \pm 0.008$
M135/147 (+5)	
- Hydrophilic	$0.246 \pm 0.026$
- Hydrophobic	$0.222 \pm 0.033$

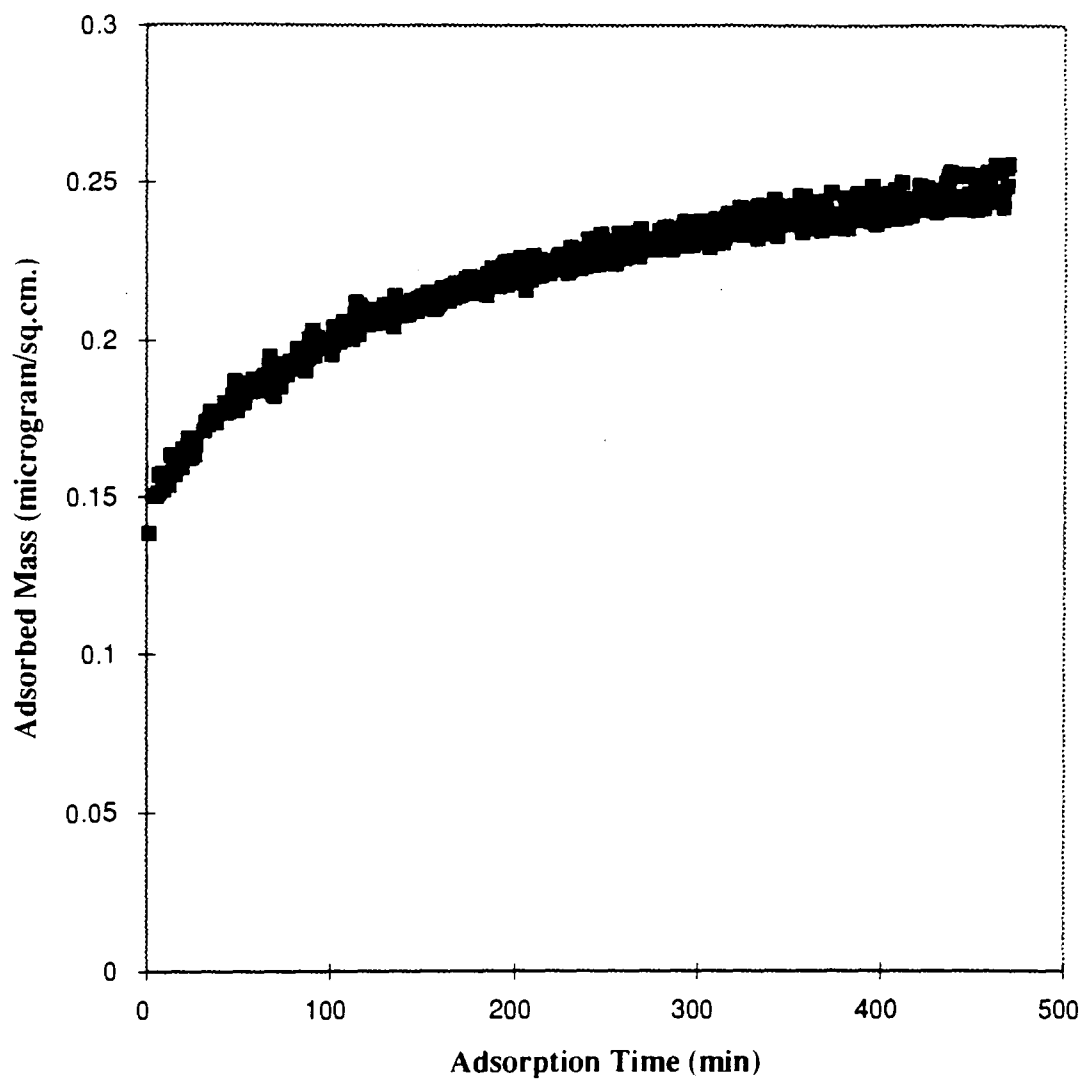


Figure 5.1. Adsorption kinetics of wild type on hydrophilic silica.

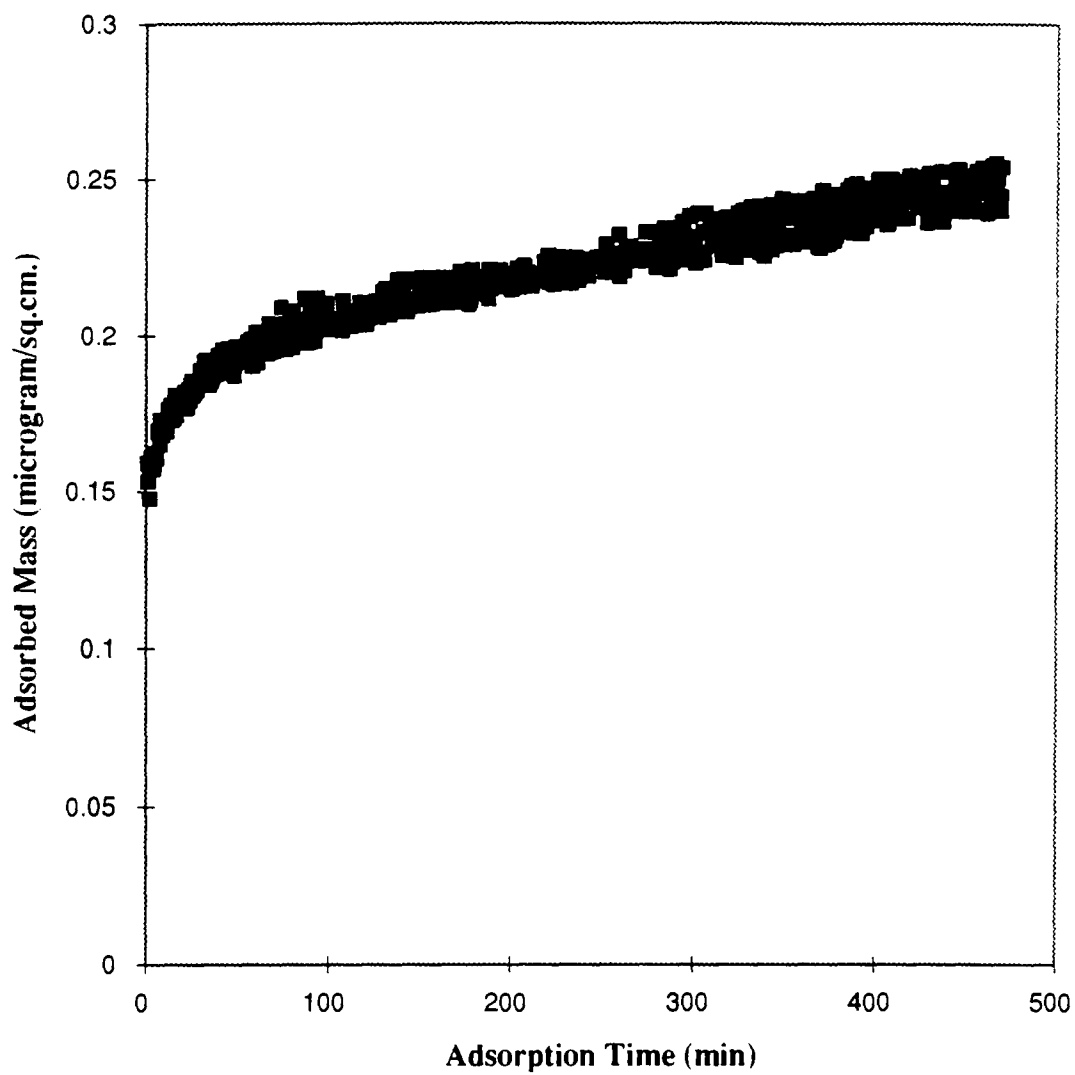


Figure 5.2. Adsorption kinetics of M135 on hydrophilic silica.



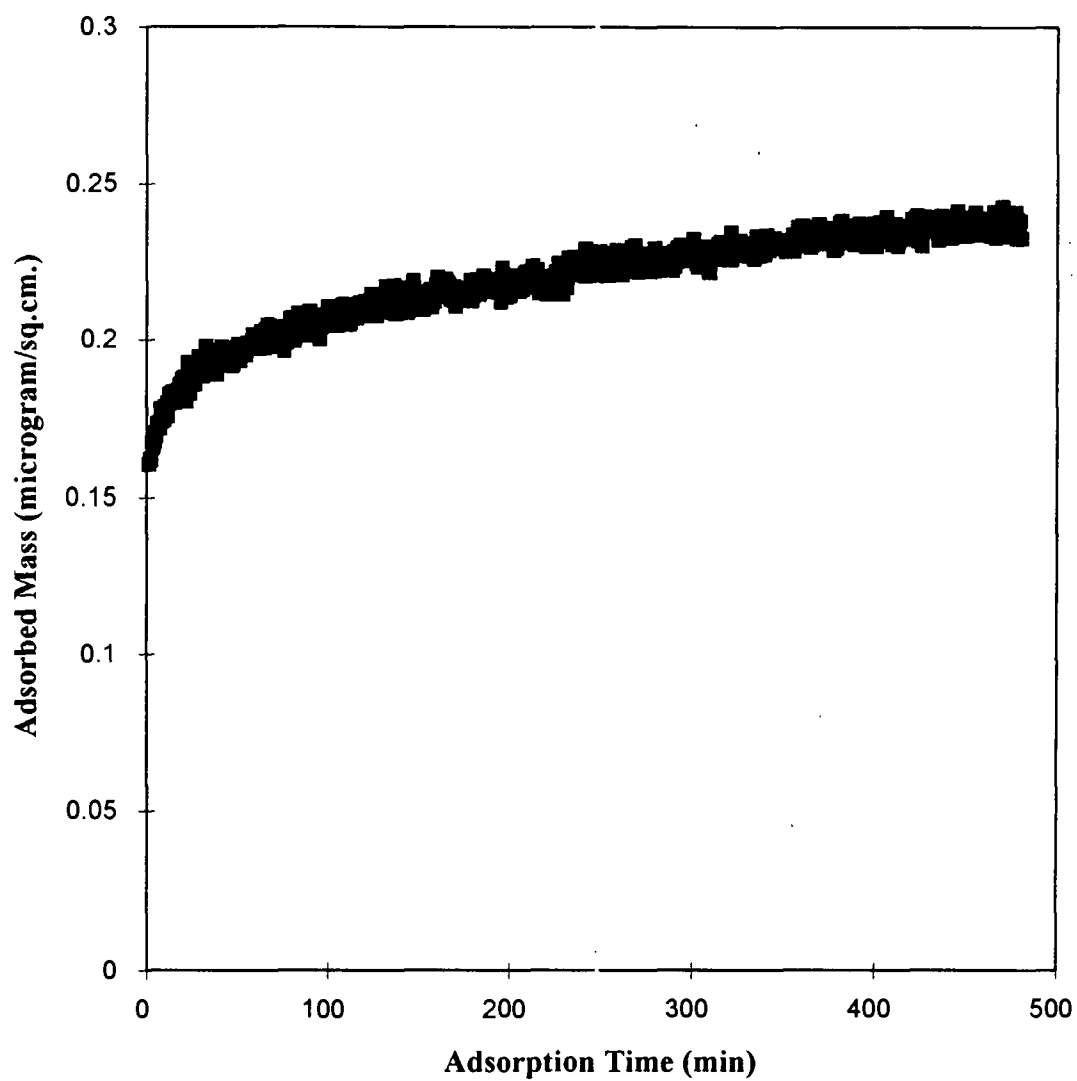


Figure 5.3. Adsorption kinetics of M135/147 on hydrophilic silica.

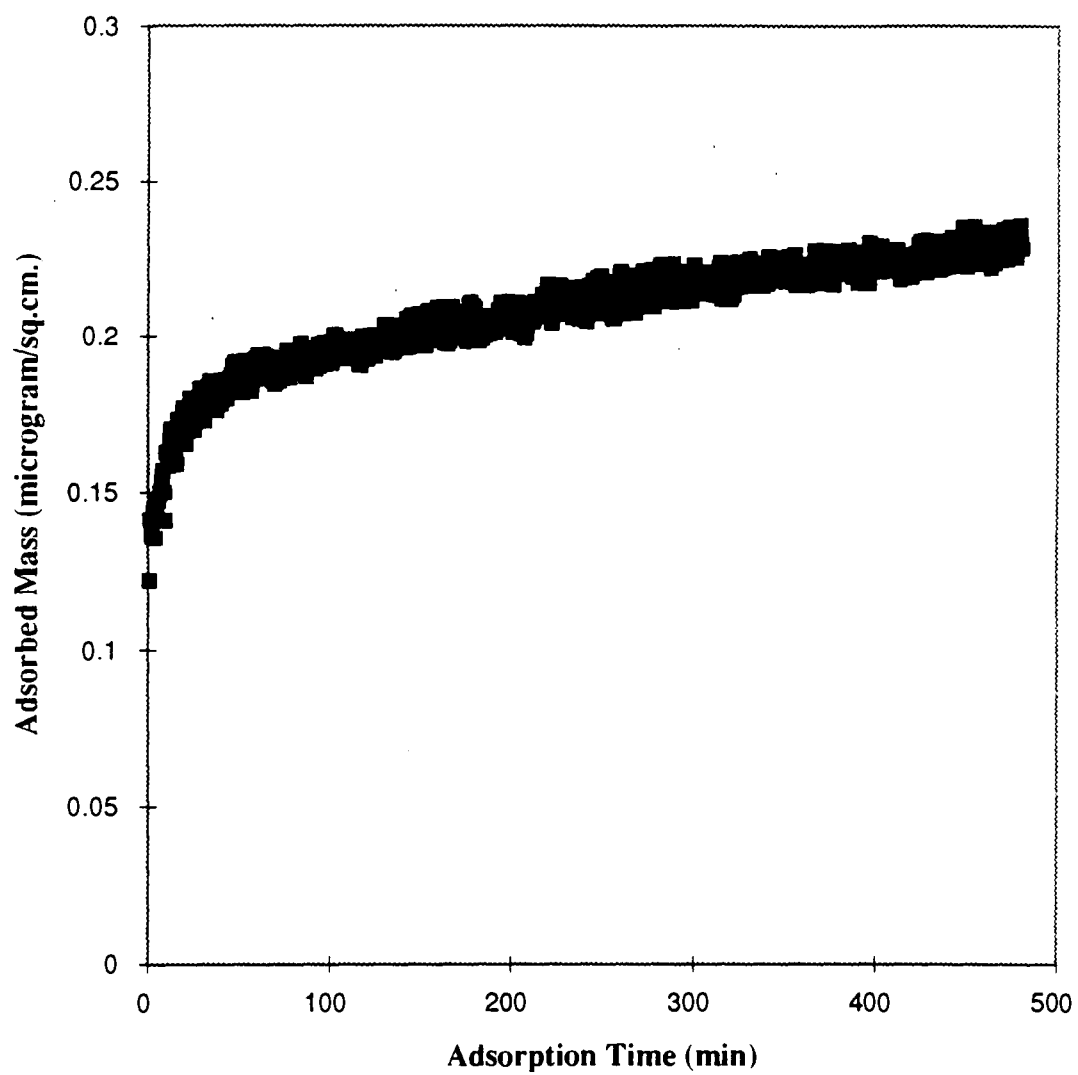


Figure 5.4. Adsorption kinetics of wild type on hydrophobic silica.

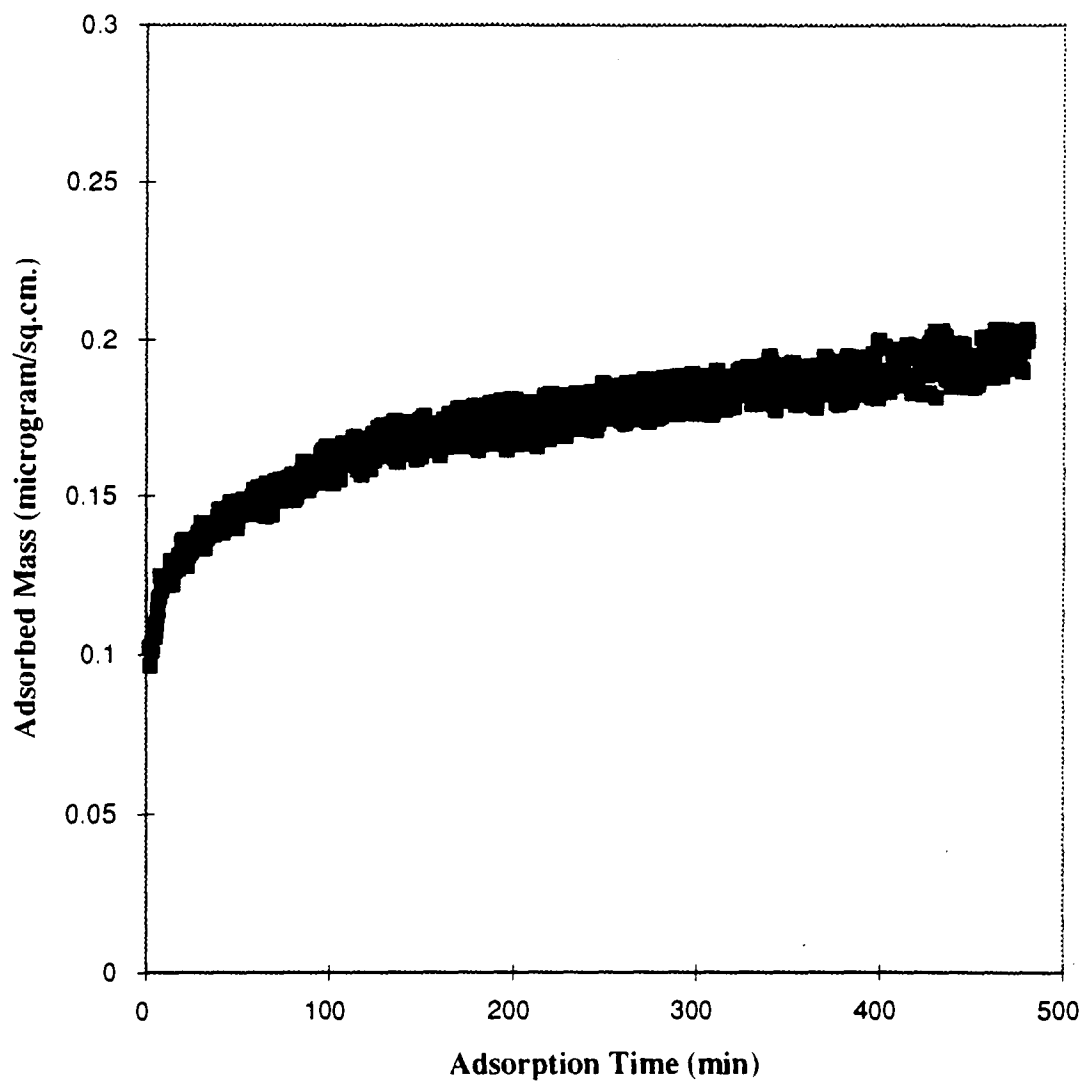


Figure 5.5. Adsorption kinetics of M135 on hydrophobic silica.

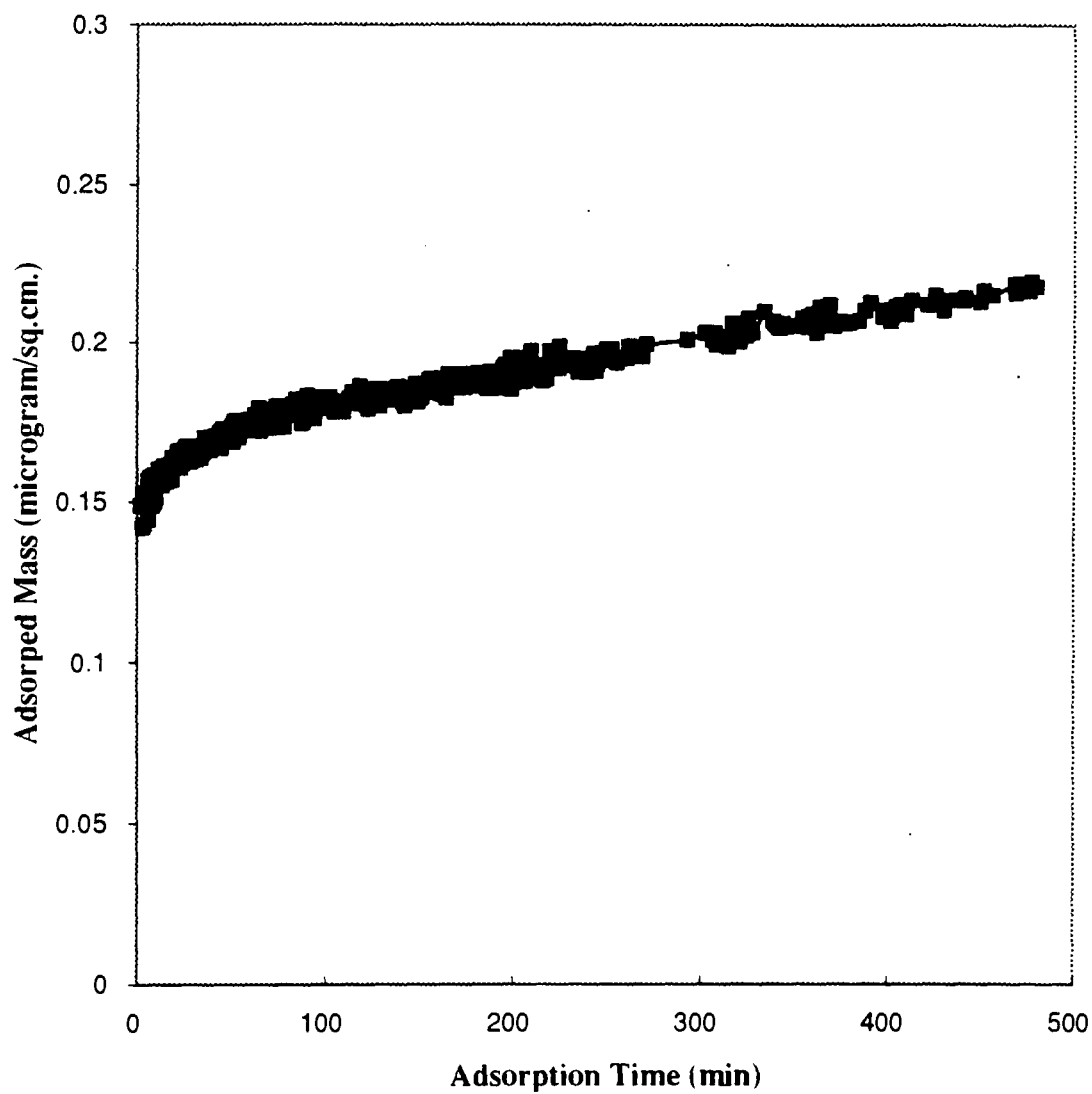


Figure 5.6. Adsorption kinetics of M135/147 on hydrophobic silica.

Representative comparisons between the pattern of adsorption kinetics recorded at hydrophilic and hydrophobic surfaces for wild type, M135, and M135/147 are shown in Figures 5.7, 5.8, and 5.9, respectively. According to Figure 5.7, wild type adsorbed on both surfaces at about the same initial rate and reached a higher apparent plateau on hydrophilic surfaces. M135 and M135/147 adsorbed much faster on hydrophilic surfaces than on hydrophobic surfaces. M135/147 attained its plateau value faster on hydrophobic surfaces, but yielded a lower adsorbed mass than at hydrophilic surfaces. In the case of M135 the plateau value was generally reached at about the same time for hydrophilic and hydrophobic surfaces, but the averaged plateau on hydrophilic surfaces is much higher than that on hydrophobic surfaces.

## **5.2 Comparison of Adsorption Kinetics on Hydrophilic and Hydrophobic Silica**

Representative comparisons between the pattern of adsorption kinetics recorded for wild type, M135, M135/147 are shown in Figure 5.10 for hydrophilic surfaces, and in Figure 5.11 for hydrophobic surfaces.

### **5.2.1 Hydrophilic Silica**

Figure 5.10 shows that M135 and M135/147 adsorbed faster than did wild type on hydrophilic surfaces, and their adsorption kinetic patterns were similar. The initial adsorption rate of M135/147 was slightly faster than that of M135. The adsorbed mass after 8h on hydrophilic surfaces, however, was greatest for wild type, followed by M135, and M135/147. This data agrees very well with the results obtained by McGuire et al. (1994a) based on kinetic data recorded for the same proteins over a period of 30 min.

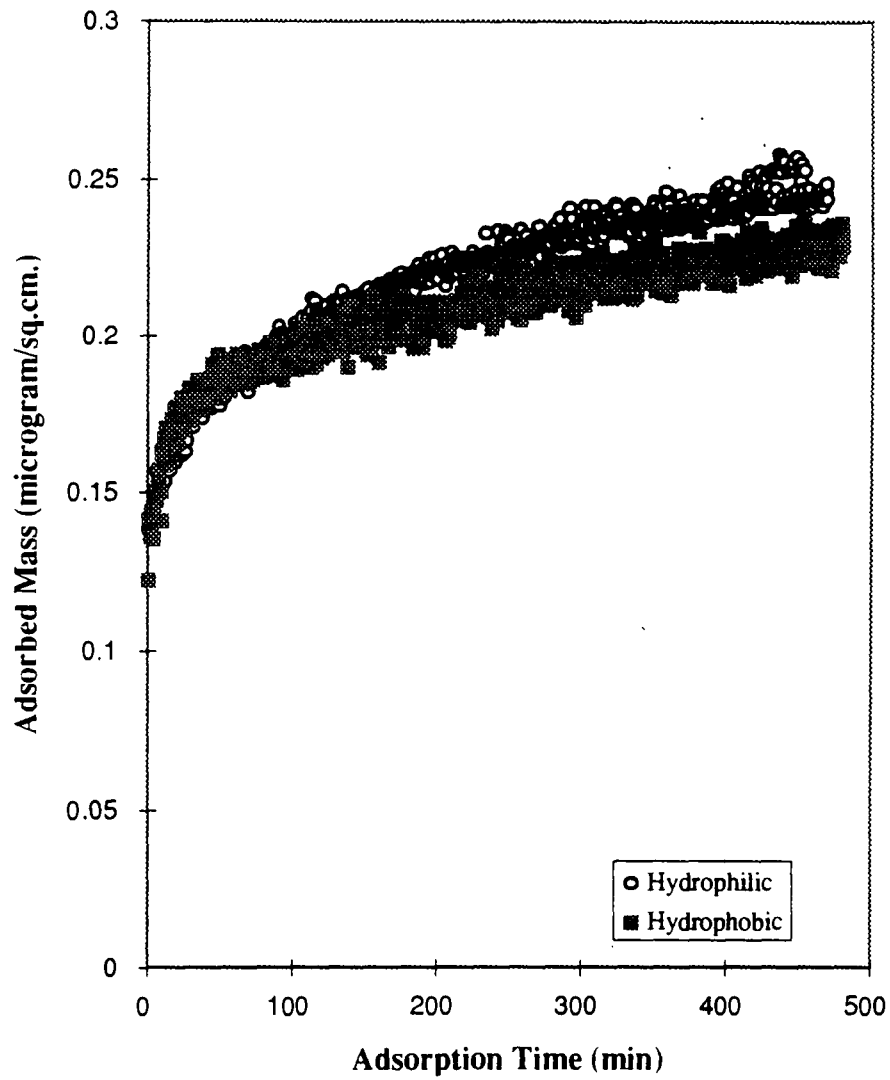


Figure 5.7. Adsorption kinetics of wild type on hydrophilic and hydrophobic silica.

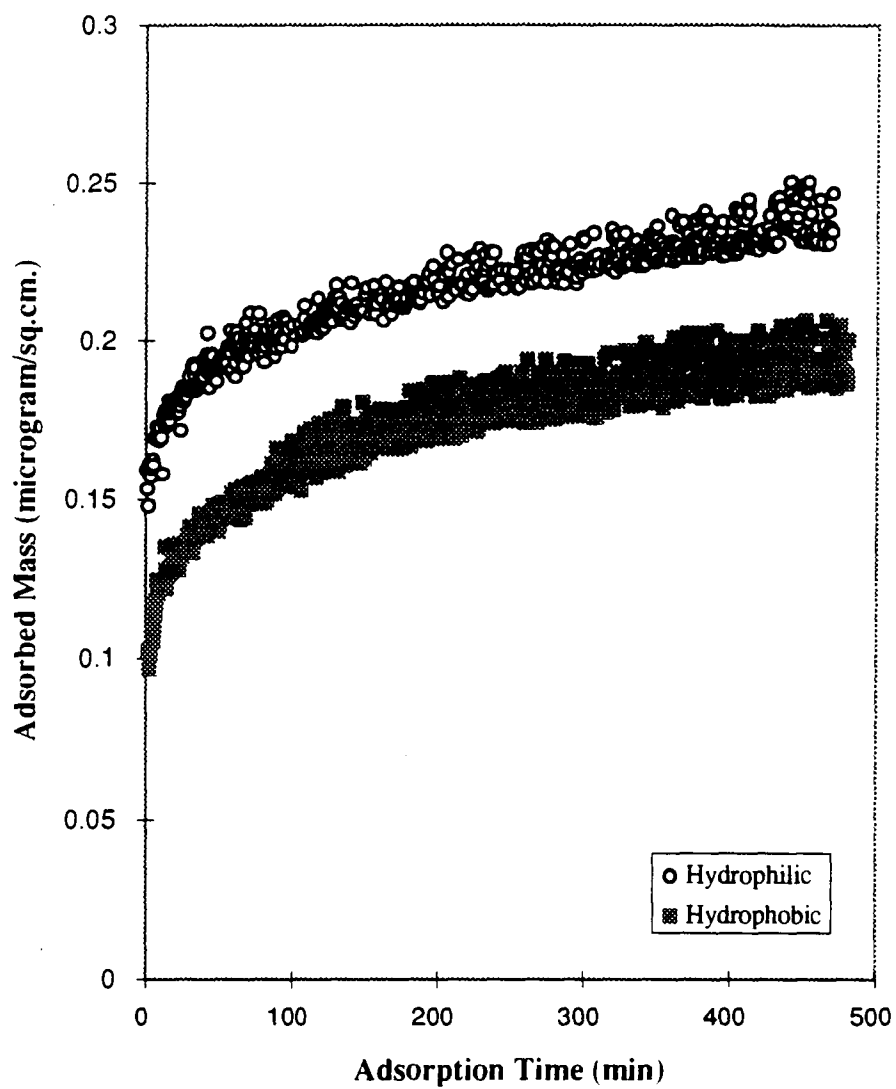


Figure 5.8. Adsorption kinetics of M135 on hydrophilic and hydrophobic silica.

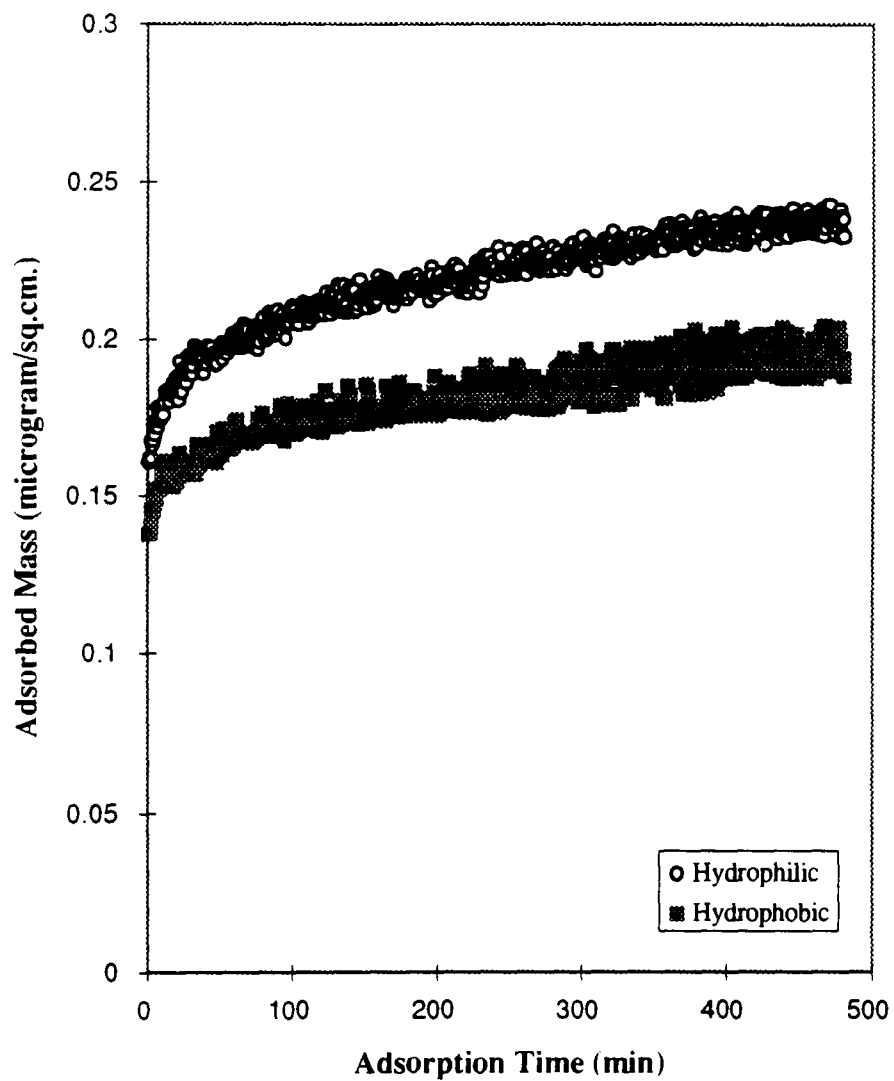


Figure 5.9. Adsorption kinetics of M135/147 on hydrophilic and hydrophobic silica.



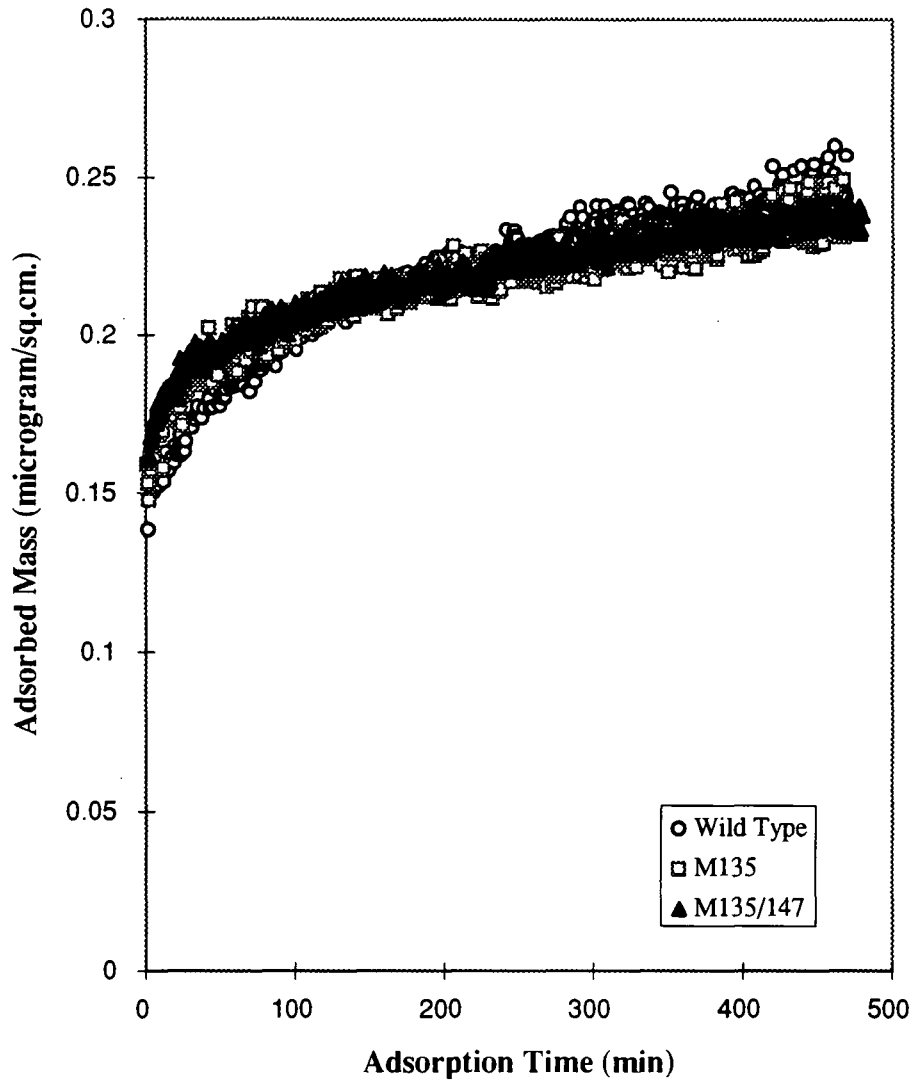


Figure 5.10. Adsorption kinetics of wild type, M135, and M135/147 on hydrophilic silica.

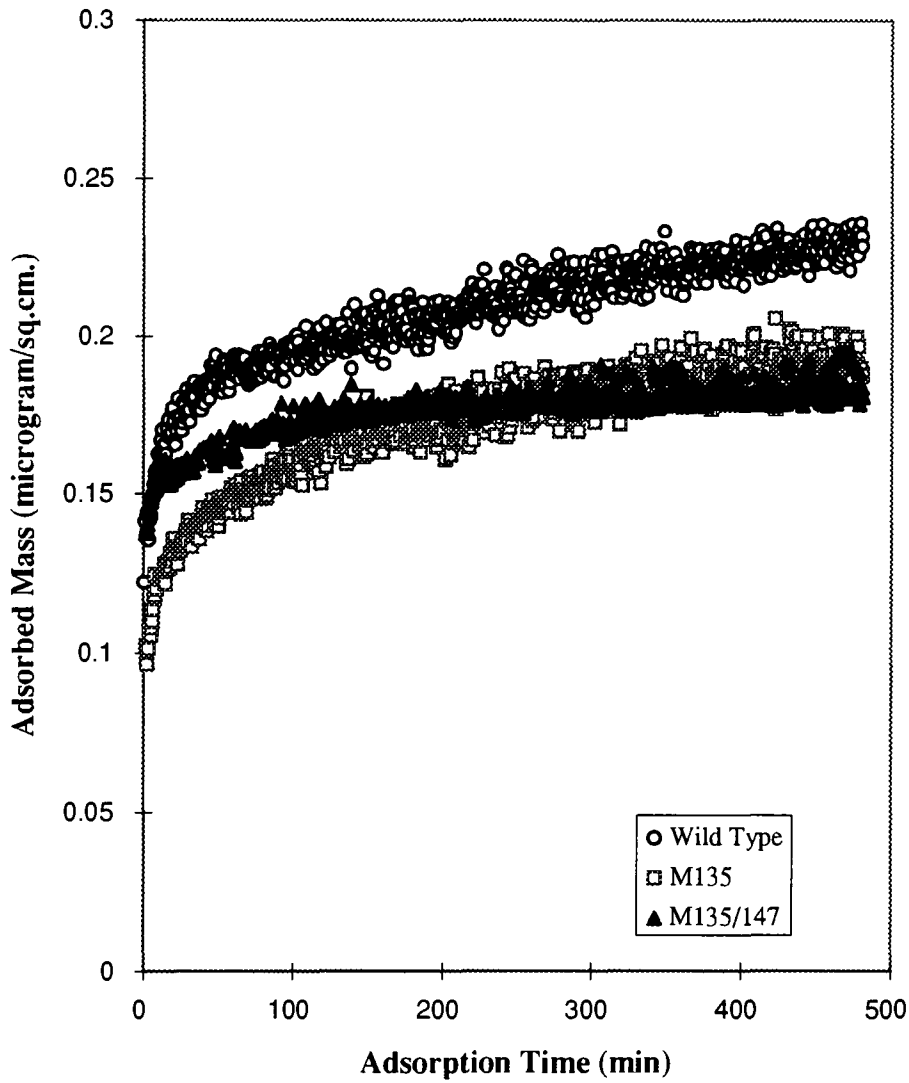


Figure 5.11. Adsorption kinetics of wild type, M135, and M135/147 on hydrophobic silica.

To most appropriately interpret the adsorption mechanisms described in Chapter 3 with regard to the T4 system, we should consider the structure of each of the variants. Table 5.2 shows that the excess of negative charges on the “back” of the C-terminal domain increases with each substitution of Lys by Glu. The back of the molecule here is defined as the furthest face of the molecule whereas the “front” of the molecule is the closest face of the molecule as depicted in Figure 3.3. Also in that figure, the active site cleft is shown on the right hand side of the  $\alpha$ -carbon backbone.

**Table 5.2.** The distribution of mobile charges for each protein (McGuire et al., 1994a).

Protein	C-terminal lobe		N-terminal lobe	
	Front	Back	Front	Back
Wild Type	+6, -1	+5, -4	+5, -2	+2, -1
M135	+6, -1	+4, -5	+5, -2	+2, -1
M135/147	+6, -1	+3, -6	+5, -2	+2, -1

McGuire et al. (1994a) hypothesized that the C-terminal lobe would first be oriented toward the negatively-charged silica surface during adsorption. They suggested that the adsorption may proceed with the most mobile regions of positive charge (the front of the C-terminal lobe) facing toward the silica surface. This orientation would allow the back of the C-terminal lobe to be oriented toward the solution. If molecules orient this

way during adsorption, weak adsorption of a second layer may occur with the front of the C-terminal lobes of molecules in the second layer facing toward the back of the C-terminal lobes of molecules in the first layer. Interaction among adsorbed molecules may be facilitated by this orientation as well, e.g., between the back of the C-terminal lobe of one molecule and the front of the N-terminal lobe of one of its neighbors, as illustrated in Figure 5.12.

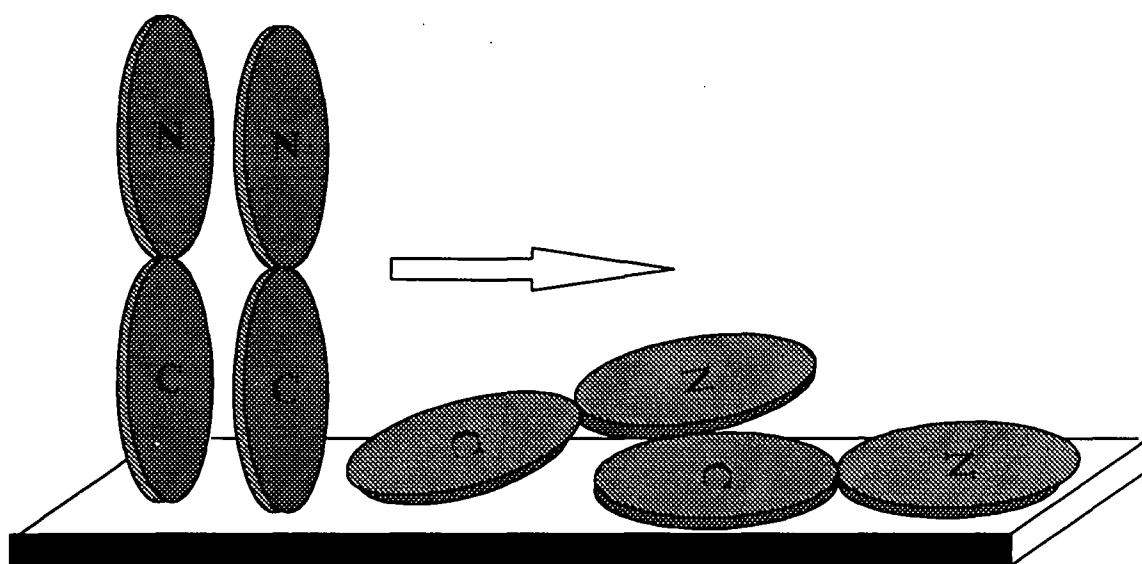


Figure 5.12. Possible adsorption behavior of T4 lysozyme on the hydrophilic surface. (McGuire et al., 1994a).

The faster initial adsorption rate at the hydrophilic surfaces exhibited by mutants of lower charge could be attributed to lower electrostatic repulsion among closely adsorbed molecules at the interface. It could also be due in part to a greater tendency for second layer formation due to a favorable electrostatic attraction afforded by the orientation shown schematically in Figure 5.12. McGuire et al. (1994a) suggested that the faster

initial adsorption kinetics of M135 and M135/147 could be partially due to enhanced second layer formation. This thinking was supported by greater rinsability exhibited by mutants of lower charge following 30 min of protein-surface contact.

**Table 5.3.** Fraction of adsorbed molecules that were rinsable following 30 min contact with hydrophilic and hydrophobic silica (McGuire et al., 1994a).

Protein	Fraction Rinsable
Wild Type (+9)	
- Hydrophilic	.162
- Hydrophobic	.104
M135 (+7)	
- Hydrophilic	.167
- Hydrophobic	.132
M135/147 (+5)	
- Hydrophilic	.246
- Hydrophobic	.142

### 5.2.2 Hydrophobic Silica

In the case of the hydrophobic surface, faster adsorption kinetics were observed for M135/147 than for M135. Wild type adsorbed faster, with a substantially greater plateau, than did M135 and M135/147. Table 5.1 shows that wild type attained the highest plateau value, on the average, followed by M135/147 and M135, respectively; again, these results are consistent with those of McGuire et al. (1994a).

Since the N-terminal lobe of T4 lysozyme has about the same number of positive and negative charges at pH 7, when compared to the C-terminal lobe, it may first be

oriented toward the hydrophobic silica surface during adsorption. T4 lysozyme may possess a hydrophobic patch opposite the active site cleft, as seen for hen and human lysozymes, which may help facilitate hydrophobic interaction with the surface. If the adsorbed molecules orient this way (side-on) during adsorption (Fig.5.14), the front and the back of the adsorbed molecules will expose to the solution. This might result in the lateral interactions among closely-adsorbed molecules. If the back of the C-terminal lobe becomes more negative, it will help decrease electrostatic repulsion between closely adsorbed molecules. Thus, more molecules with greater excess of mobile, negative charges at the back of the C-terminal lobe will adsorb in this side-on manner than molecules with less excess of mobile, negative charges. This explains why M135 and M135/147 attained lower plateaus than did wild type.

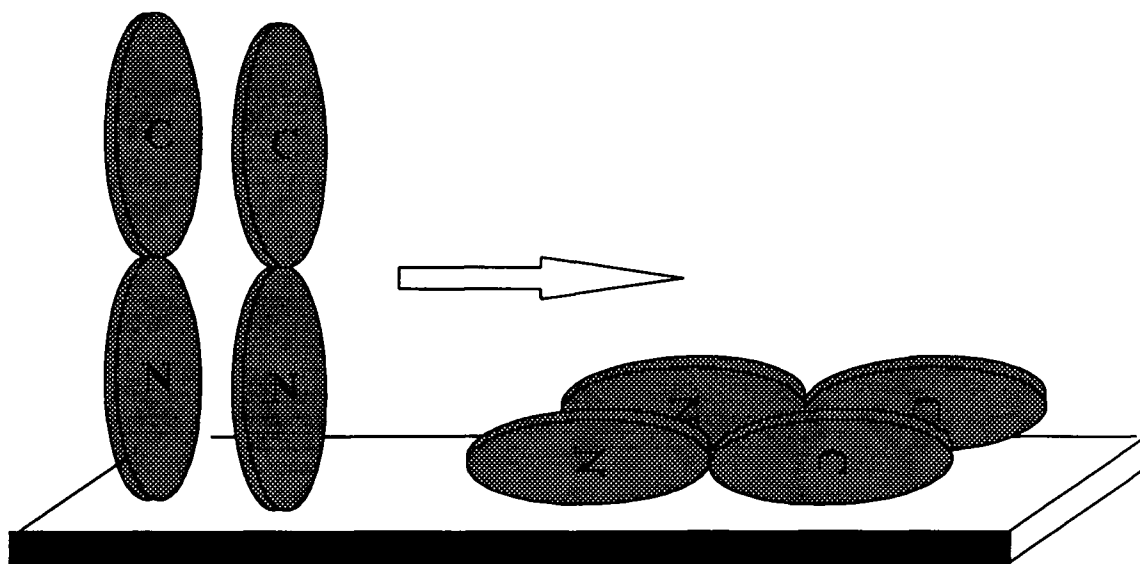


Figure 5.13. Possible adsorption behavior of T4 lysozyme on the hydrophobic surface.

## 5.3 Comparison to Kinetic Models

### 5.3.1 Three-rate-constant model (model 1)

We originally hypothesized that bacteriophage T4 lysozyme would adsorb according to the simple kinetic model described by Krisdhasima et al. (1992b). That model was analyzed under each of three conditions. First,  $s_1$  was assumed constant among wild type and all charge mutants, while  $k_1$  and  $k_{-1}$  could differ. Second,  $k_1$  and  $k_{-1}$  were assumed constant instead of  $s_1$ . The third, condition allowed all kinetic rate constants to be variable.

#### 5.3.1.1 Condition 1

In this case it was assumed that  $s_1$  was mainly dependent on the stability of the proteins. Since the stability of each protein was similar,  $s_1$  could be assumed constant. Unlike  $s_1$ ,  $k_1$  and  $k_{-1}$  were expected to vary, depending on electrostatic interactions between the protein and surface. By fitting Eq. [4] to the experimental data, parameters  $r_1$  and  $r_2$ , known functions of  $k_1$ ,  $k_{-1}$ , and  $s_1$  according to Eqs. [5] and [6] were estimated from each run. After performing a t-test for determining 95% confidence interval, five  $s_1$  values from a similar kinetic study focused on T4 lysozyme stability mutants (Singla, 1994) were selected for each type of surfaces (0.4322, 0.4530, 0.4843, 0.5009, and 0.5415 for hydrophilic surfaces; and 0.2434, 0.2473, 0.2910, 0.3083, and 0.3434 for hydrophobic surfaces), based on 95% confidence interval (see Appendix C). Values of  $k_1C$ ,  $k_{-1}$ , and  $k_{-1}/k_1C$  for each protein on each type of surface were calculated separately

for each run according to Eqs. [5] and [6], using each  $s_1$ ,  $r_1$ , and  $r_2$  combination allowable for a given run. Then, the average values of  $k_{-1}/k_1C$  for each protein on each type of surfaces were estimated and are shown in Table 5.4.

**Table 5.4.** Values of the ratio  $k_{-1}/k_1C$  obtained by analysis of kinetic data with Eqs. [5] and [6], holding  $s_1$  constant.

Protein	$k_{-1}/k_1C$
Wild Type (+9)	
- Hydrophilic	41.25
- Hydrophobic	38.72
M135 (+7)	
- Hydrophilic	56.27
- Hydrophobic	19.36
M135/147 (+5)	
- Hydrophilic	64.93
- Hydrophobic	26.54

The ratio  $k_{-1}/k_1C$  indicates the tendency of molecules to leave the surface during the period preceding surface-induced conversion to an irreversibly bound form. In the case of hydrophilic surfaces, this ratio increased as the net charge of the protein decreased. This is consistent with expectations based solely on the effect of electrostatic interaction between charges of the protein molecules and charges on the surface. Because hydrophilic silica surfaces possess some negative charge, the greater the number of



positive charges on the protein molecule, the greater the electrostatic attraction with the surface.

On hydrophobic surfaces, hydrophobic association is expected to dominate in protein adsorption. Therefore, the lower the charge, the lower the  $k_{-1}/k_1C$  since electrostatic repulsion between the adsorbed protein and its neighbors are minimized. According to Table 5.4,  $k_{-1}/k_1C$  is lower on hydrophobic surfaces on the average. This agrees with what should be expected. The  $k_{-1}/k_1C$  seems to drop as the charge of the protein is reduced. However, we cannot see a very clear relationship between  $k_{-1}/k_1C$  and the net charge of proteins on hydrophobic surfaces.

When looking at the  $k_{-1}/k_1C$  ratio alone this kinetic model might seem to explain the effects of protein charge on its adsorption in terms of expectations based on electrostatic interactions, but it does not agree with the adsorption kinetic pattern of each protein exhibited in this research. In the case of hydrophilic surfaces, according to Figure 5.10, the initial adsorption rate increased as the net charge of the protein decreased whereas the  $k_{-1}/k_1C$  ratio suggested that the adsorption rate decrease as the net charge of the protein decreased. Moreover, comparison plots between adsorption kinetics of proteins on hydrophilic and hydrophobic surfaces (Figures 5.7, 5.8, and 5.9) show that proteins adsorbed faster on hydrophilic surfaces, which is opposite to what the data of Table 5.4 would predict.

### 5.3.1.2 Condition 2

This time  $k_1$ , and  $k_{-1}$  were assumed constant and unaffected by protein charges, as opposed to  $s_1$ , which was allowed to vary among the mutants. The kinetic rate constants were estimated by solving Eqs. [5] and [6] for all dissimilar protein pair combinations allowable. Each pair combination yields a set of four equations and four unknowns. Then, the average  $s_1$  was estimated for each protein on each type of surface, and the average  $k_1$  and  $k_{-1}$  were calculated for hydrophilic and hydrophobic surfaces (Appendix D). Averaged  $s_1$ ,  $k_1$ , and  $k_{-1}$  values are shown in Table 5.5.

**Table 5.5.** Values of the rate constants  $k_1$ ,  $k_{-1}$ , and  $s_1$  obtained by analysis of kinetic data with Eqs. [5] and [6], holding  $k_1$  and  $k_{-1}$  constant.

Surface	Protein	$s_1$	$k_1 C$	$k_{-1}$
Hydrophilic	Wild Type	0.586	$1.492 \times 10^{-2}$	0.299
	M135	1.463		
	M135/147	0.927		
Hydrophobic	Wild Type	0.590	$1.010 \times 10^{-2}$	0.498
	M135	0.698		
	M135/147	1.007		

Table 5.5 shows that the forward adsorption rate constant ( $k_1 C$ ) is higher on hydrophilic surfaces than on hydrophobic surfaces whereas the desorption rate constant ( $k_{-1}$ ) is higher on hydrophobic surfaces. This would be consistent with the adsorption

kinetic patterns of Figures 5.7 to 5.9. The value of  $s_1$  increases with decreasing protein charge on hydrophobic surfaces. Despite the fact that  $s_1$  on hydrophilic surfaces is higher for M135 than for M135/147, overall  $s_1$  increased with a substitution of lysine by glutamic acid at these sites. This interpretation of model 1 is thus more realistic than that described earlier; i.e., a surface-induced conversion -at least one similar in concept to that shown in Figure 5.12- is apparently affected by the location of particular charges in the molecule. Moreover, neither the protein's net charge nor its stability was clearly related to post-adsorption behavior.

### 5.3.1.3 Condition 3

All rate constants were assumed to be affected by the protein charges and were allowed to be variable. Parameters  $r_1$  and  $r_2$  from each run were obtained by fitting Eq.[4] to experimental data (Appendix E). The averaged  $r_1$  and  $r_2$  were calculated for each protein on each type of surface. Then  $s_1 k_1 C$  was calculated according to Eq. [6], using the averaged  $r_1$  and  $r_2$  as shown in Table 5.6.

The value of  $s_1 k_1 C$  increases with decreasing protein charge on hydrophobic surfaces. The increase in  $s_1 k_1 C$  can be the result of either an increase in  $s_1$  and/or  $k_1$ . The adsorption kinetic patterns shown in Figure 5.11 would be consistent with a decrease in  $k_1$  in the order  $k_{1, \text{wild type}} > k_{1, \text{M135/147}} > k_{1, \text{M135}}$ , according to results of simulation of Eq. [4] by Krisdhasima et al. (1992a). Therefore, the increase in  $s_1 k_1 C$  in this case must involve an increase in  $s_1$ . In any event, structural rearrangement and/or molecular

re-orientation of adsorbed molecules on the hydrophobic surfaces appears to increase as the net charge of protein decreases. With this increase, the number of molecules in an irreversibly adsorbed forms would increase. This is consistent with the elutability data obtained by McGuire et al. (1994a) where M135/147 exhibited the lowest elutability by DTAB, followed by M135 and wild type.

**Table 5.6.** Averaged values of  $r_1$  and  $r_2$  for each protein-surface contact, and the corresponding values of  $s_1k_1C$  for each case, calculated according to Eq. [6].

Surface	Protein	$r_1(\times 10^3)$	$r_2$	$s_1k_1C \times 10^2$
Hydrophilic	Wild Type (+9)	6.78	1.11	0.75
	M135 (+7)	6.70	2.28	1.53
	M135/147 (+5)	6.15	1.42	0.87
Hydrophobic	Wild Type (+9)	6.40	0.97	0.62
	M135 (+7)	8.10	0.84	0.68
	M135/147 (+5)	8.63	1.13	0.98

In the case of hydrophilic surfaces, there is an increase in  $s_1k_1C$  value when there is a substitution of Lys by Glu. Figure 5.10 would indicate that there is not any substantial change in  $k_1$  when the net charge of the protein was reduced, and the increase in  $s_1k_1C$  accompanying reduction of the net charge probably involved an increase in  $s_1$ .

### 5.3.2 Parallel adsorption model (Model 2)

McGuire et al. (1994b) suggested that T4 lysozyme molecules adsorbed in different states occupy different interfacial areas. They proposed a kinetic model based on a mechanism where molecules can directly adsorb from solution onto a surface in one of two different states. These two states of adsorbed molecules showed different resistances to elution by DTAB. State 2 molecules exhibited greater resistance to elution than did state 1 molecules. The present data were analyzed with reference to this model by a non-linear regression and a linear regression analysis.

#### 5.3.2.1 Non-linear regression analysis

By fitting the experimental data to Eq. [11] using non-linear regression analysis,  $k_1C$ ,  $k_2C$ , and  $k_2/k_1$  were calculated for each run (Appendix F). Averaged values of  $k_2/k_1$  are shown in Table 5.7. This ratio would provide an indication of the number of molecules that are more tightly bound (state 2) relative to the number of molecules that are less tightly bound (state 1). The more molecules in state 2 (i.e., the higher the value of  $k_2/k_1$ ), the lower the plateau value expected in the associated kinetic plot, since state 2 molecules occupy a greater interfacial area than do state 1 molecules.

Table 5.7 shows that  $k_2/k_1$  decreased with protein net charge at hydrophilic surfaces. This is opposite to that expected based on the plateau values recorded in

Table 5.1. At hydrophobic surfaces as well, the correlation between  $k_2/k_1$  and the associated plateau values was not completely evident, although  $k_2/k_1$  was always higher for a given protein at hydrophobic than at hydrophilic surfaces, as required.

**Table 5.7.** Averaged values of  $k_2/k_1$  obtained by non-linear regression analysis of kinetic data with Eq. [11].

Protein	$k_2/k_1$
Wild Type (+9)	
- Hydrophilic	2.62
- Hydrophobic	7.99
M135 (+7)	
- Hydrophilic	2.23
- Hydrophobic	12.56
M135/147 (+5)	
- Hydrophilic	1.64
- Hydrophobic	4.80

In summary, the relative magnitudes of the plateau values are not consistent with the  $k_2/k_1$  ratios, and the data of Table 5.7 are neither reflective of the kinetic data nor consistent with any plausible aspects of the previous discussion concerning model 1. The reason for this stems from attempting to fit these kinetic plots to a single-exponent function, especially in cases where the kinetic plot is characterized by a rather low initial slope, attaining no obvious plateau after 8h (Figure 5.14).

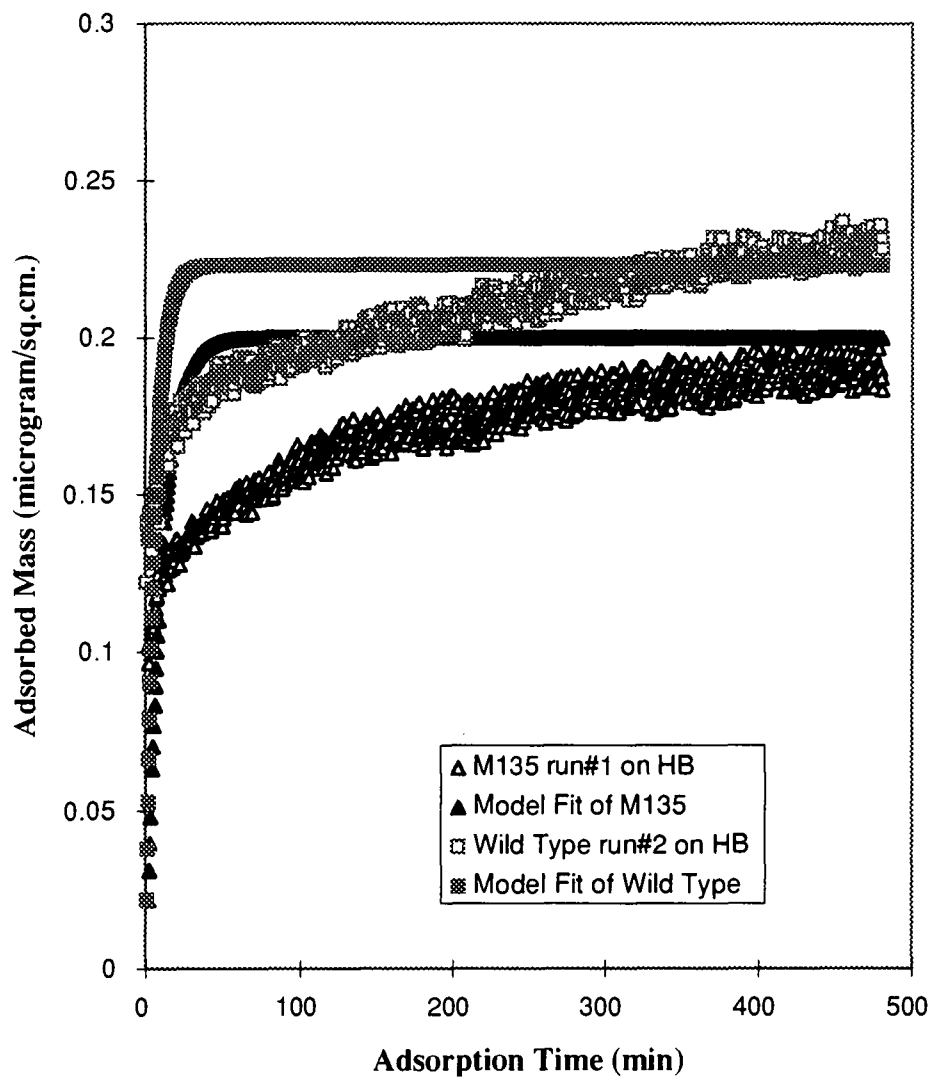


Figure 5.14. Comparison plots between model fitting and experimental data.

### 5.3.2.2 Linear regression analysis

In order to better represent the patterns of kinetic data, they were analyzed by a linear regression analysis to better fit the plateau regions. For this purpose, experimental data were divided into two parts: the initial contact time, between 0 and 60 min., and the contact time between 61 and 480 min. This is because the relationship between adsorbed mass and time between 0 and 60 min. is exponential while the relationship between adsorbed mass and time for the rest of the time duration is more or less linear. Linear regression analysis was performed on the data for the period 61 to 480 min. For each run, the slope of the kinetic plot between 61 and 480 min. along with the adsorbed mass observed after 8h. were used in the calculation of  $k_1C$  and  $k_2C$ . From Eq.[11],

$$\Gamma = \Gamma_{\max} \cdot \frac{(1 + k_2/k_1)}{1 + ak_2/k_1} \cdot [1 - \exp(-k_1C - ak_2C)t]$$

or  $\Gamma = \Gamma_{\text{plateau}} \cdot [1 - \exp(-k_1C - ak_2C)t]$ .

After rearranging the above equation we got

$$\ln(\Gamma_{\text{plateau}} - \Gamma) = \ln(\Gamma_{\text{plateau}}) - (k_1C + ak_2C)t.$$

By plotting  $\ln(\Gamma_{\text{plateau}} - \Gamma)$  vs.  $t$  on semilog scales,  $k_1C$  and  $k_2C$  were calculated from

$$\text{slope} = -(k_1C + ak_2C)t$$

and  $\Gamma_{\text{plateau}} = \Gamma_{\max} \cdot \frac{(1 + k_2/k_1)}{1 + ak_2/k_1}$ .

The ratio  $k_2/k_1$  was then calculated from  $k_1C$  and  $k_2C$  estimated for each run (Appendix G). The averaged values of  $k_2/k_1$  for each protein on each type of surface was calculated and shown in Table 5.8.



Table 5.8 shows that on hydrophilic surfaces values of  $k_2/k_1$  of wild type and M135 are similar while  $k_2/k_1$  of M135/147 is highest. This would imply that more molecules adopt the more tightly bound form as charge is decreased to +5 units. This result is in general agreement with the plateau values shown in Table 5.1 as well. The highest  $k_2/k_1$  ratio on hydrophobic surfaces was obtained for M135, followed by M135/147 and wild type. This is also in general agreement with the plateau value data. Finally, the  $k_2/k_1$  ratio is higher for adsorption on hydrophobic surfaces for all proteins, as required since plateau values were lower on these surfaces than on hydrophilic surfaces for each protein.

**Table 5.8.** Averaged values of  $k_2/k_1$  obtained by linear regression analysis of kinetic data with Eq. [11].

Protein	$k_2/k_1$
Wild Type (+9)	
- Hydrophilic	1.25
- Hydrophobic	2.93
M135 (+7)	
- Hydrophilic	1.26
- Hydrophobic	4.16
M135/147 (+5)	
- Hydrophilic	1.79
- Hydrophobic	3.83

According to Table 5.8, proteins apparently adsorb at these interfaces more tightly and occupy a greater interfacial area with substitution of Lys with Glu. With reference to

model 1,  $s_1$  would increase with substitution of Lys with Glu on both hydrophilic and hydrophobic surfaces. This suggests that the mutants undergo structural rearrangement and/or re-orientation faster than the wild type. In short, results from both models point to the same conclusion that the replacement of Lys by Glu facilitates the adsorption of T4 lysozyme. This is apparently not related to changes in net charge, but to the locations of the substitutions allowing more rapid attainment of the states possibly similar to that shown as the final form in Fig. 5.12 for hydrophilic surfaces and in Fig. 5.13 for hydrophobic surfaces.

## CHAPTER 6

### CONCLUSION

When there is a substitution of Lys with Glu proteins apparently adsorb at both hydrophilic and hydrophobic interfaces more tightly and occupy a greater interfacial area than does wild type. Results from the three-rate-constant and the parallel adsorption models point to the same conclusion that the replacement of Lys by Glu facilitates the adsorption of T4 lysozyme. This is apparently not related to changes in net charge, but to the locations of the substitutions allowing more rapid attainment of the final adsorbed states possibly similar to the face-on adsorption for hydrophilic surfaces and side-on adsorption for hydrophobic surfaces.

## BIBLIOGRAPHY

- Alber, T. and B.W. Matthews. 1987. Structure and thermal stability of phage T4 lysozyme., *Meth. Enzymol.* **154**:511-533.
- Al-Makhlafi, H., J. McGuire, and M. Daeschel. 1994. Influence of preadsorbed milk proteins on adhesion of *Listeria monocytogenes* to hydrophobic and hydrophilic silica surfaces., *Appl. Environ. Microbiol.* **60**:3560-3565.
- Andrade, J.D. 1985. Surface and Interfacial Aspects of Biomedical Polymers. Volume 2: Protein adsorption, J.D. Andrade (ed.), p.1, Plenum Press, New York.
- Andrade, J.D., V.L. Hlady, and R.A. Van Wagenen. 1984. Effects of plasma protein adsorption on protein conformation and activity., *Pure Appl. Chem.* **56**: 1345-1350.
- Arai, T. and W. Norde. 1990a. The behavior of some model proteins at solid-liquid interfaces I : Adsorption from single protein solutions., *Colloid and Surfaces.* **51**:1-15.
- Arai, T. and W. Norde. 1990b. The behavior of some model proteins at solid-liquid interfaces II : Sequential and competitive adsorption., *Colloid and Surfaces.* **51**:17-28.
- Arnebrant T., B. Ivarsson, K. Larsson, I. Lundstrom, and T. Nylander. 1985. Bilayer formation at adsorption of proteins from aqueous solutions on metal surfaces. *Progr. Colloid Polymer Sci.* **70**:62-66.
- Arnebrant T. and T. Nylander. 1988. Adsorption of insulin on metal surfaces in relation to association behavior., *J. Colloid Interface Sci.* **122**:557-566.
- Bohnert, J.L. and T.A. Horbett. 1986. Changes in adsorbed fibrinogen and albumin interactions with polymers indicated by decreases in detergent elutibility., *J. Colloid Interface Sci.* **111**:363-377.
- Bryers, J.D. 1987. Biologically active surfaces : Processes governing the formation and persistence of biofilms, *Biotechnol. Prog.* **3(2)**:57-68.
- Criado, M-T., B. Suárez, and C.M. Ferreirós. 1994. The importance of bacterial adhesion in the dairy industry., *Food Technol.* **Feb**:123-126.

- Daeschel, M.A., J. McGuire, and H. Al-Makhlafi. 1992. Antimicrobial activity of nisin adsorbed to hydrophilic and hydrophobic silicon surfaces., *J. Food Prot.* **55**: 731-735.
- Dao-pin, S., E. Soderlind, W.A. Baase, J.A. Wozniak, U. Sauer, and B.W. Matthews. 1992. Cumulative site-directed charge-change replacements in bacteriophage T4 lysozyme suggest that long-range electrostatic interactions contribute little to protein stability., *J. Mol. Biol.* **221(3)**:873-887.
- DeFeijter, J.A., J. Benjamins, and F.A. Veer. 1978. Ellipsometry as a tool to study the adsorption behavior of synthetic and biopolymers at the air-water interface., *Biopolymers* **17**:1759-1772.
- Elbaum, D., J. Harrington, E.F. Roth, and R.L. Nagel. 1976. Surface activity of hemoglobin S and other human hemoglobin variants., *Biochem. Biophys. Acta.* **427**:57-69.
- Elgersma, A.V., R.L.J. Zsom, J. Lyklema, and W. Norde. 1992. Adsorption competition between albumin and monoclonal immuno-gamma-globulins on polystyrene lattice., *J. Colloid Interface Sci.* **152(2)**:410-428.
- Grütter, M.G., R.B. Hawkes, and B.W. Matthews. 1979. Molecular basis of thermostability in the lysozyme from bacteriophage T4., *Nature* **277**:67-669.
- Grütter, M.G. and B.W. Matthews. 1982. Amino acid substitutions far from the active site of bacteriophage T4 lysozyme reduce catalytic activity and suggest that the C-terminal lobe of the enzyme participates in substrate binding., *J. Mol. Biol.* **154**: 525-535.
- Grütter, M.G., L.H. Weaver, T.M. Gray, and B.W. Matthews. 1983. Structure, function, and evolution of the lysozyme from bacteriophage T4. *in* Bacteriophage T4. p.356-360. (eds. Mathews, C.K., E.M. Kutter, G. Mosig, and P.M. Berget) Am. Soc. Microbiology., Wahington, D.C.
- Horbett, T.A. 1988. Molecular origins of the surface activity of proteins., *Protein Eng.* **2**:172-174.
- Jönsson, U., I. Lunström, and I. Rönnberg. 1987. Immunoglobulin G and secretory fibronectin adsorption to silica., *J. Colloid Interface Sci.* **117**:127-138.
- Kato, A., and K. Yutani. 1988. Correlation of surface properties with conformational stabilities of wild-type and six mutant tryptophan synthase  $\alpha$ -subunits substituted at the same position., *Protein Eng.* **2**:153-156.

- Kondo, A. and K. Higashitani. 1992. Adsorption of model proteins with wide variation in molecular properties on colloidal particles., *J. Colloid Interface Sci.* **150(20)**: 344-351.
- Kornberg, A., and T.A. Baker. 1992. DNA Replication. 2<sup>nd</sup> ed. W.H. Freeman and Company, NY.
- Krisdhasima, V., J. McGuire, and R.D. Sproull. 1992a. A one-film-model ellipsometry program for the simultaneous calculation of protein film thickness and refractive index., *Surf. Interface Anal.* **18**:453-456.
- Krisdhasima, V., J. McGuire, and R.D. Sproull. 1992b. Surface hydrophobic influences on  $\beta$ -lactoglobulin adsorption kinetics., *J. Colloid Interface Sci.* **154(2)**:337-350.
- Krisdhasima, V., P. Vinaraphong, and J. McGuire. 1993. Adsorption kinetics and elutibility of  $\alpha$ -lactalbumin,  $\beta$ -casein,  $\beta$ -lactoglobulin, and bovine serum albumin at hydrophobic and hydrophilic interfaces., *J. Colloid Interface Sci.* **161**: 325-334.
- Luey, J-K., J. McGuire, and R.D. Sproull. 1991. The effect of pH and NaCl concentration on adsorption of  $\beta$ -lactoglobulin at hydrophilic and hydrophobic silicon surfaces., *J. Colloid Interface Sci.* **143(2)**:489-499.
- Lundström, I. 1985. Models of protein adsorption on solid surfaces., *Progr. Colloid Polymer Sci.* **70**:76-82.
- Lundström I., and H. Elwing. 1990. Simple kinetic model for protein exchange reactions on solid surfaces., *J. Colloid Interface Sci.* **136**:68-84.
- Matsumura, M., W.J. Bechtel, and B.W. Matthews. 1988. Hydrophobic stabilization in T4 lysozyme determined directly by multiple substitutions of Ile 3., *Nature* **334**: 406-410.
- Matsumura, M., and B.W. Matthews. 1989. Control of enzyme activity by an engineered disulfide bond., *Science* **243**:792-794.
- Matthews, B.W., F.W. Dahlquist, and A.Y. Maynard. 1973. Crystallographic data for lysozyme from bacteriophage T4., *J. Mol. Biol.* **78**:575-576.
- Matthews, B.W. and S.J. Remington. 1974. The three dimensional structure of the lysozyme from bacteriophage T4., *Proc. Nat. Acad. Sci., U.S.A.* **71**:4178-4182.

- McGuire, J., V. Krisdhasima, M.C. Wahlgren, and T. Arnebrant. 1994c. Comparative adsorption studies with synthetic, structural stability and charge mutants of bacteriophage T4 lysozyme. in Proteins at Interfaces, J. Brash and T. Horbett, eds., ACS Books, Washington, D.C., **in press**.
- McGuire, J., M.C. Wahlgren, and T. Arnebrant. 1994a. The influence of net charge and charge location on the adsorption and dodecyltrimethylammonium bromide-mediated elutability of bacteriophage T4 lysozyme at silica surfaces., *J. Colloid Interface Sci.* **in press**.
- McGuire, J., M.C. Wahlgren, and T. Arnebrant. 1994b. Structural stability effects on the adsorption and dodecylammonium bromide-mediated elutability of bacteriophage T4 lysozyme at silica surfaces., *J. Colloid Interface Sci.* **in press**.
- Norde, W. and A.C.I. Anusiem. 1992. Adsorption, desorption, and re-adsorption of proteins on solid surfaces., *Colloids Surf.* **66(1):73-80**.
- Norde, W. and J.P. Favier. 1992. Structure of adsorbed and desorbed protein., *Colloid Surf.* **64(2):87-93**.
- Norde, W. and I. Lyklema. 1978a. The adsorption of human plasma albumin and bovine pancrease ribonuclease at negatively charged polystyrene surface I : Adsorption isotherms; effect of charge, ionic strength, and temperature., *J. Colloid Interface Sci.* **66(2):257-265**.
- Norde, W. and I. Lyklema. 1978b. The adsorption of human plasma albumin and bovine pancrease ribonuclease at negatively charged polystyrene surface II : Hydrogen ion titrations., *J. Colloid Interface Sci.* **66(2):266-276**.
- Norde, W. and I. Lyklema. 1978c. The adsorption of human plasma albumin and bovine pancrease ribonuclease at negatively charged polystyrene surface IV : The charge distribution in the adsorbed states., *J. Colloid Interface Sci.* **66(2):285-294**.
- Shirahama, H., J. Lyklema, and W. Norde. 1990. Competitive protein adsorption in model system., *J. Colloid Interface Sci.* **139(1) 177-186**.
- Singla, B. 1994. Adsorption of selected stability mutants of bacteriophage T4 lysozyme at silanized silica surface. Master's thesis. Department of Chemical Engineering, Oregon State University, Corvallis, OR.
- Remington, S.J., W.F. Anderson, J. Owen, L.F. Ten Eyck, C.T. Grainger, and B.W. Matthews. 1978. Structure of lysozyme from bacteriophage T4 : an electron density map at 2.4 Å resolution., *J. Mol. Biol.* **118:81-98**.

- Soderquist, M.E. and A.G. Walton. 1980. Structural changes in proteins adsorbed on polymer surface., *J. Colloid Interface Sci.* **75**:386-397.
- Suttiprasit, P., V. Krisdhasima, and J. McGuire. 1992. The surface activity of  $\alpha$ -lactalbumin,  $\beta$ -lactoglobulin, and bovine serum albumin I : Surface tension measurements with single-component and mixed solutions., *J. Colloid Interface Sci.* **154**:316-326.
- Suttiprasit, P. and J. McGuire. 1992. The surface activity of  $\alpha$ -lactalbumin,  $\beta$ -lactoglobulin, and bovine serum albumin II : Some molecular influences on adsorption to hydrophillic and hydrophobic silicon surfaces., *J. Colloid Interface Sci.* **154**:327-336.
- Tosteson, T.R., and W.A. Corpe. 1975. Enhancement of adhesion of the marine *Chlorella vulgaris* to glass., *Can J. Microbiol.* **21**:1025-1031.
- Voet, D., and Judith G. Voet. 1990. Biochemistry. John Wiley & Sons, Inc. New York.
- Wahlgren, M. and T. Arnebrant. 1990. Adsorption of  $\beta$ -lactoglobulin onto silica, methylated silica, and polysulfone., *J. Colloid Interface Sci.* **136**:259-265.
- Walton, A.G. and F.C. Maenpa. 1979. Application of fluorescence spectroscopy to the study of protein at interfaces., *J. Colloid Interface Sci.* **72**:265-278.
- Weaver, L.H. and B.W. Matthews. 1987. Structure of bacteriophage T4 lysozyme refined at 1.7 Å resolution., *J. Mol. Biol.* **193**:189-198.
- Xu, S., and S. Damodaran. 1993. Comparative adsorption of native and denatured egg-white, human, and T4 phage lysozymes at the air-water interfaces., *J. Colloid Interface Sci.* **159**:124-133.
- Zubay, G. 1983. Biochemistry. Addison-Wesley Publishing Company, Inc. Reading, MA.



## **APPENDICES**

## APPENDIX A

## M/A ratios and specific volumes of each protein

M/A ratios and specific volumes of each protein are calculated according to the primary structure of each protein. The numbers shown in Table A.1 are used in the calculation of  $r_1$  and  $r_2$  by OEP program.

**Table A.1.** M/A ratios and the specific volumes of each protein used in OEP program.

Protein	M/A ( $\mu\text{gm}/\text{cm}^2$ )	Specific volume ( $\text{cm}^3/\mu\text{gm}$ )
Wild Type	3.827	0.780
M135	3.832	0.780
M135/147	3.838	0.778

## APPENDIX B

## Preparation of broths, buffers, and solutions

Recipes for preparation of overnight broth and fermentation broth are shown in Table B.1. Buffers and solutions used in this research are made according to recipes in Table B.2.

**Table B.1.** Preparation of LB broth (overnight broth) and LB-H broth (fermentation broth)

Ingredients	LB broth	LB-H broth
Tryptone(g)	57.6	2.0
NaCl (g)	48.0	1.0
Yeast extract (g)	24.0	1.0
Glucose (g)	4.8	0.0
Distilled water (L)	4.8	0.2
1N NaOH (mL)	0.0	0.2

**Table B.2.** Preparation of buffers and solutions.

Buffers/Solutions	pH	Preparation
0.5 M EDTA	8.0	14.61 g EDTA / 100 mL DDW use NaOH pellet to adjust pH to 7.2 at 80°C, then cool down and add DDW or 1N NaOH to 100 mL and adjust pH to 8.0
10 mM HCl		0.1 mL HCl / 120 mL DDW
1.0 M MgCl <sub>2</sub>		20.33 g MgCl <sub>2</sub> / 100 mL DDW
0.1 M Phosphate buffer	6.5	0.7112 g mono + 1.3785 g di-phosphate + 0.03 g NaN <sub>3</sub> + 4.8213 g NaCl in 150 mL DDW
10 mM Phosphate buffer	7.0	2.2078 g mono in 1600 mL DDW titrate with 3.5490 g di in 2500 mL DDW to pH 7.0, then add 0.8 g NaN <sub>3</sub>
50 mM Phosphate buffer	5.8	25.0866 g mono + 2.5840 g di-phosphate in 4 L DDW + 0.8 g NaN <sub>3</sub>
Lysis buffer	6.6	2.0699 g mono + 1.4196 g di-phosphate + 2.9220 g NaCl + 0.5083 g MgCl <sub>2</sub> in 250 mL DDW
10 mM Tris buffer	7.4	0.1322 g Tris acid + 0.0914 g Tris base in 100 mL DDW
50 mM Tris buffer	7.25	6.49 g Tris acid + 0.74 g Tris base in 1 L DDW
50 mM NaCl in Tris		1.2272 g NaCl / 420 mL 50 mM Tris
0.3 M NaCl in Tris		7.8894 g NaCl / 450 mL 50 mM Tris

## APPENDIX C

Averaged values of kinetic rate constants from the three-rate-constant model, assuming  $k_1$  and  $k_{-1}$  are depending on electrostatic interaction between the protein and the surface.

From a similar study focused on T4 lysozyme stability mutants (wild type vs. Trp), 9 values of  $s_1$  for hydrophilic surfaces and 11 values of  $s_1$  for hydrophobic surfaces were obtained (Singla, 1994). After performing a t-test for determining 95% confidence interval, the 95% confidence interval was used to eliminate data points that do not fall within the limits.

Five  $s_1$  values were selected for each type of surfaces (0.4322, 0.4530, 0.4843, 0.5009, and 0.5415 for hydrophilic surfaces; and 0.2434, 0.2473, 0.2910, 0.3083, and 0.3434 for hydrophobic surfaces), based on 95% confidence interval. Values of  $k_1C$ ,  $k_{-1}$ , and  $k_{-1}/k_1C$  for each protein on each type of surface were calculated separately for each run according to Eqs. [5] and [6], using each  $s_1$ ,  $r_1$ , and  $r_2$  combination allowable for a given run. Then, the average values of  $k_{-1}/k_1C$  for each protein on each type of surfaces were estimated and are shown in Table C.1 to C.6.

### Determining 95% confidence interval

For a small sample size, confidence interval equals  $x_{av} \pm t_{critical} \cdot (s/n^{1/2})$ , when  $s$  is the standard deviation and  $n$  is the sample size.

### **Hydrophilic surfaces**

$s_1 = 0.4530, 0.4322, 0.4843, 0.3708, 0.4289, 0.5009, 0.6054, 0.5415, \text{ and } 0.5979.$

$x_{av} = 0.4905$  and  $s = 0.0749.$

At 95% confidence level and d.f. = 8,  $t = 2.31$ , the 95% confidence interval is equal  $[0.4905 - (0.0749/3), 0.4905 + (0.0749/3)]$  or  $[0.4294, 0.5516]$ .

### Hydrophobic surfaces

$s_1 = 0.6204, 0.2434, 0.3083, 0.0218, 0.1594, 0.9548, 0.0532, 0.3434, 0.8788, 0.2910,$   
and  $0.2473$ .

$x_{av} = 0.3747$  and  $s = 0.3116$ .

At 95 % confidence level and d.f. = 10,  $t = 2.23$  and the confidence interval is  $[0.1678, 0.6072]$ .

**Table C.1.** Averaged values of  $k_1$ ,  $k_{-1}$ , and the ratio  $k_{-1}/k_1C$  of wild type on hydrophilic silica.

$s_1$	$k_1C \times 10^2$	$k_{-1}$	$k_{-1}/k_1C$
0.4530	2.0309	0.9982	49.1506
	2.2517	0.8348	37.0742
	0.8300	0.3666	44.1687
0.4322	2.1286	1.0180	47.8249
	2.3600	0.8545	36.2076
	0.9255	0.3840	41.7504
0.4843	1.8996	0.4167	21.9362
	2.1061	0.8049	38.2176
	0.8259	0.3353	40.5981
0.5009	1.8367	0.9522	51.8430
	2.0363	0.7890	38.7467
	0.7986	0.3190	39.9467
0.5415	1.6993	0.9130	53.7280
	1.8840	0.7500	39.8089
	0.7377	0.2790	37.7691
average			41.2514

**Table C.2.** Averaged values of  $k_1$ ,  $k_{-1}$ , and the ratio  $k_{-1}/k_1C$  of M135 on hydrophilic silica.

$s_1$	$k_1C \times 10^2$	$k_{-1}$	$k_{-1}/k_1C$
0.4530	3.4437	2.4007	69.7128
	3.0243	1.3752	45.4717
	3.3775	1.6206	47.9822
0.4322	3.6094	2.4198	57.0416
	3.1698	1.3945	43.9933
	3.5400	1.6398	46.3220
0.4843	3.2211	2.3716	73.6270
	2.8288	1.3458	47.5749
	3.1592	1.5915	50.3767
0.5009	3.1144	2.3561	75.6518
	2.7351	1.3301	48.6308
	3.0545	1.5760	51.5960
0.5415	2.8814	2.3178	80.4401
	2.5305	1.2916	51.0413
	2.8255	1.5376	54.4187
average			56.2674

**Table C.3.** Averaged values of  $k_1$ ,  $k_{-1}$ , and the ratio  $k_{-1}/k_1C$  of M135/147 on hydrophilic silica.

$s_1$	$k_1C \times 10^2$	$k_{-1}$	$k_{-1}/k_1C$
0.4530	1.9205	1.2090	62.9524
	1.1479	0.6175	53.7939
	2.4945	1.7924	71.5841
0.4322	2.0130	1.2289	61.0482
	1.2031	0.6378	53.0130
	2.6145	1.8120	69.3058
0.4843	1.7964	1.1789	65.6257
	1.0737	0.5870	54.6708
	2.3333	1.7627	75.5454
0.5009	1.7369	1.1629	66.9526
	1.0381	0.5707	54.9754
	2.2559	1.7468	77.4325
0.5415	1.6069	1.1236	10.2772
	0.9605	0.5309	55.2733
	2.0872	1.7079	81.8273
average			64.9283



**Table C.4.** Averaged values of  $k_1$ ,  $k_{-1}$ , and the ratio  $k_{-1}/k_1C$  of wild type on hydrophobic silica.

$s_1$	$k_1C \times 10^2$	$k_{-1}$	$k_{-1}/k_1C$
0.2434	1.5612	0.5531	35.4279
	1.7666	0.6254	35.4013
	3.6976	1.2701	34.3493
0.3083	1.2326	0.4915	39.8751
	1.3947	0.5643	40.4603
	2.9192	1.2188	41.7512
0.3434	1.1066	0.4576	41.3519
	1.2522	0.5306	42.3734
	2.6209	1.1867	45.2783
0.2910	1.3058	0.5080	38.9034
	1.4777	0.5807	39.2976
	3.0928	1.2344	39.9121
0.2473	1.5366	0.5494	35.7543
	1.4777	0.5807	39.2976
	3.6393	1.2726	34.9683
average			38.7243

**Table C.5.** Averaged values of  $k_1$ ,  $k_{-1}$ , and the ratio  $k_{-1}/k_1C$  of M135 on hydrophobic silica.

$s_1$	$k_1C \times 10^2$	$k_{-1}$	$k_{-1}/k_1C$
0.2434	2.5062	0.4504	17.9714
	1.5201	0.2708	17.8146
	2.4240	0.4866	20.0743
0.3083	1.9786	0.3908	19.7513
	1.2001	0.2091	17.4235
	1.9137	0.4268	22.3023
0.3434	1.7764	0.3577	20.1362
	1.0775	0.1752	17.3896
	1.7181	0.3936	22.9090
0.2910	2.0962	0.4069	19.4113
	1.2715	0.2257	17.7507
	2.0275	0.4429	21.3446
0.2473	2.4666	0.4469	18.1181
	1.4962	0.2671	17.8519
	2.3858	0.4830	20.2448
average			19.3662

**Table C.6.** Averaged values of  $k_1$ ,  $k_{-1}$ , and the ratio  $k_{-1}/k_1C$  of M135/147 on hydrophobic silica.

$s_1$	$k_1C \times 10^2$	$k_{-1}$	$k_{-1}/k_1C$
0.2434	2.2597	0.8298	36.7218
	6.7790	1.0775	15.8947
	3.4100	0.6660	19.5308
0.3083	1.7840	0.7497	42.0235
	5.3519	1.0269	19.1876
	2.6921	0.6083	22.5957
0.3434	1.6016	0.7164	44.7303
	4.8049	0.9973	20.7559
	2.4170	0.5759	23.8271
0.2910	1.8900	0.7659	40.5238
	5.6701	1.0410	18.3595
	2.8522	0.6240	21.8778
0.2473	2.2240	0.8063	36.2545
	6.6721	1.0747	16.1074
	3.3562	0.6626	19.7426
average			26.5422

## APPENDIX D

Averaged values of kinetic rate constants from the three-rate-constant model, assuming  $k_1$  and  $k_{-1}$  are unaffected by protein charges.

Assuming  $k_1$  and  $k_{-1}$  are the same for all mutants and wild type, values of  $s_1$ ,  $k_1C$ , and  $k_{-1}$  are calculated directly from  $r_1$  and  $r_2$  values, according to Eqs. [5] and [6]. Only all positive results are recorded for each pair of data used in calculation. The 95% confidence interval is used to eliminate data points that do not fall within the limits. Then, average values of  $s_1$ ,  $k_1C$ , and  $k_{-1}$  are calculated and shown in Table D.1 to Table D.4.

**Table D.1.** Averaged  $s_1$  values for each protein on hydrophilic surfaces.

	Wild Type	M135	M135/147
$s_1$	0.1034 1.1429 0.4993 0.0596 0.7996 0.9623 0.8855 0.7999 0.3175 0.4649 0.7203 0.4300 0.4567 0.7349 0.6391	1.1865 1.5982 2.7421 2.7044 2.7805 1.4605 1.7362 0.4872 1.2472 0.9877 1.5472	0.4960 0.2366 1.5882 2.0815 1.5352 0.8983 0.3100 0.4708 0.5615 0.5218 0.8741 1.7510 1.9598 1.4733 1.1619 0.7715
n	15	11	16
average $s_1$	0.6011	0.7614	1.0432
d.f.	14	10	15
t	2.15	2.23	2.13
s.d.	0.306814	0.5119	0.6110
upper limit	0.7714	2.1917	1.3792
lower limit	0.4308	1.1679	0.7072
adjusted n	6	6	4
adjusted average $s_1$	0.5859	1.4626	0.9265

**Table D.2.** Averaged  $s_1$  values for each protein on hydrophobic surfaces.

	Wild Type	M135	M135/147
$s_1$	0.5377 0.5433 0.2629 0.1719 0.6007 0.1125 0.2697 0.4791 0.6121 1.2875 0.6192 0.2784 0.1778 0.7169 0.0630 1.2233 1.2890	0.1546 0.7853 0.2928 0.4823 1.3526 0.6781 0.3930 0.6482 0.3811 0.3780 0.2487 0.3400 0.5993 0.3521 0.4791 0.5755 1.3846 0.6059 1.2420 1.2385	0.8442 0.7485 0.8644 0.2439 1.2233 0.6800 0.9062 0.1201 0.7428 1.0627 0.8728 0.4674 0.8867 1.1080 0.7541 0.9866 0.6684 0.2579 0.9347 0.1545 0.4415
n	17	20	21
average $s_1$	0.5438	0.6306	0.7128
d.f.	16	19	20
t	2.120	2.093	2.086
s.d.	0.3978	0.3798	0.3184
upper limit	0.7484	0.8083	0.8577
lower limit	0.3393	0.4529	0.5679
adjusted n	7	8	6
adjusted average $s_1$	0.5870	0.6067	0.7397

**Table D.3.** Averaged values of kinetic rate constants for lysozyme on hydrophilic silica.

	$k_1 C \times 10^2$	$k_{-1}$
	6.7636	0.7006
	0.8077	0.3205
	1.1545	0.6604
	0.9593	0.4996
	1.0424	0.5756
	1.2701	0.4977
	2.1853	0.8235
	0.5598	0.1020
	0.9379	0.3885
	0.8830	0.3624
	0.5488	0.0875
	0.6310	0.1825
	0.5677	0.1403
	0.5756	0.1780
	2.8116	1.3431
	1.0983	0.6002
	1.5522	1.1042
	0.9909	0.5503
	0.5916	0.2020
	0.7501	0.5118
	0.6702	0.3038
n	21	21
average	1.3024	0.4826
s.d.	1.3728	0.3250
d.f.	20	20
t	2.09	2.09
upper limit	1.9440	0.6345
lower limit	0.6608	0.3307
adjusted n	12	8
adjusted average	1.0097	0.4983

**Table D.4.** Averaged values of kinetic rate constants for lysozyme on hydrophobic silica.

	$k_1 C \times 10^2$	$k_{-1}$
	0.7057	0.2673
	0.6985	0.2618
	1.4433	0.5347
	2.2070	0.6181
	0.6317	0.2051
	3.3718	0.6658
	2.3992	0.3509
	1.3505	0.1519
	0.9731	0.2604
	0.9810	0.5926
	1.4910	0.6844
	1.0908	0.1636
	0.9838	0.7549
	1.6745	0.3257
	1.2306	0.2240
	2.1171	0.3104
	0.8800	0.0318
	3.5346	0.0613
	1.8632	0.1386
	0.6977	0.1416
	1.5515	0.2658
	2.4294	0.1785
	0.6026	0.1451
	6.8518	0.3854
	0.7351	0.2628
	1.2666	0.7967
	0.9008	0.8860
	1.5545	0.4834
	0.9425	$2.9823 \times 10^{-8}$
n	29	29
average	1.6262	0.3450
s.d.	1.2648	0.2437
d.f.	28	28
t	2.048	2.048
upper limit	2.1072	0.4426
lower limit	1.1452	0.2573
adjusted n	9	9
adjusted average	1.4917	0.2989



## APPENDIX E

Values of the kinetic model parameters from the three-rate-constant model

The parameters  $r_1$  and  $r_2$  are directly determined by non-linear regression analysis of the experimental data fit to the kinetic model 1, suggested by Krisdhasima et al.

(1992b) Values of each of these parameters are shown in Table E.1 and E.2.

**Table E.1.** Values of the kinetic model parameters from the three-rate-constant model for each protein on hydrophilic surfaces.

Protein	Run #	Date of Exp.	$-r_1$	$-r_2$
Wild Type	1	11/01/93	0.0081	0.8636
	2	12/12/93	0.0063	1.4652
	3	12/14/93	0.0078	1.3025
	4	12/30/93	0.0049	0.8230
M135	1	12/31/93	0.0054	2.8827
	2	01/14/94	0.0074	1.8510
	3	04/16/94	0.0073	2.1001
M135/147	1	01/03/94	0.0052	1.6760
	2	01/04/94	0.0088	0.6535
	3	01/05/94	0.0048	1.0773
	4	01/07/94	0.0058	2.2645

**Table E.2.** Values of the kinetic model parameters from the three-rate-constant model for each protein on hydrophobic surfaces.

Protein	Run#	Date of Exp.	$-r_1$	$-r_2$
Wild Type	1	01/25/94	0.0047	0.8074
	2	02/01/94	0.0102	0.6343
	3	02/08/94	0.0049	0.8816
	4	02/13/94	0.0058	1.5505
M135	1	01/18/94	0.0071	0.5223
	2	01/20/94	0.0079	0.7463
	3	01/27/94	0.0088	1.3846
	4	02/12/94	0.0086	0.7103
M135/147	1	04/07/94	0.0051	1.0707
	2	06/28/94	0.0120	1.3767
	3	06/29/94	0.0088	0.9347

## APPENDIX F

Values of the kinetic model parameters from the parallel adsorption model, using non-linear regression analysis

The parameters  $k_1C$  and  $k_2C$  are directly determined by non-linear regression analysis of the experimental data fit to the kinetic model suggested by McGuire et al. (1994b). In this research, the values of  $A_2/A_1$  on hydrophilic and hydrophobic silica surfaces have been modified to 2.11 and 1.99, respectively. These new values were obtained from the experimental data observed in this research. Values of each of parameters  $k_1, k_2$ , and  $k_2/k_1$  are shown in Table F.1 and Table F.2.

**Table F.1.** Values of the kinetic model parameters from the parallel adsorption model for each protein on hydrophilic surfaces, using non-linear regression analysis.

Protein	Run #	Date of Exp.	$k_1$	$k_2$	$k_2/k_1$
Wild Type	1	11/01/93	0.0094	0.0151	1.61
	2	12/12/93	0.0075	0.0157	2.09
	3	12/14/93	0.0087	0.0535	6.15
	4	12/30/93	0.2230	0.1403	0.63
M135	1	12/31/93	0.4883	0.3976	0.81
	2	01/14/94	0.0542	0.1739	3.21
	3	04/16/94	0.0783	0.2099	2.68
M135/147	1	01/03/94	0.0425	0.0470	1.11
	2	01/04/94	0.0004	0.0281	70.25*
	3	01/05/94	0.0466	0.1247	2.68
	4	01/07/94	0.0102	0.0114	1.12

**Table F.2.** Values of the kinetic model parameters from the parallel adsorption model for each protein on hydrophobic surfaces, using non-linear regression analysis.

Protein	Run #	Date of Exp.	$k_1$	$k_2$	$k_2/k_1$
Wild Type	1	01/25/94	0.0082	0.0734	8.95
	2	02/01/94	0.0004	0.1760	440*
	3	02/08/94	0.0087	0.0774	8.90
	4	02/13/94	0.0055	0.0337	6.13
M135	1	01/18/93	0.0069	0.0338	4.90
	2	01/20/94	0.0022	0.0474	21.55
	3	01/27/94	0.0058	0.1322	22.79
	4	02/12/94	0.0295	0.0295	1.00
M135/147	1	04/07/94	0.0237	0.1782	7.52
	2	06/28/94	0.0650	0.3241	4.99
	3	06/29/94	0.0317	0.0596	1.88

\* Remark : Run #2 of M135/147 on hydrophilic surfaces and run #2 of wild type on hydrophobic surfaces will not be used in the calculation of average  $k_2/k_1$  because they are significantly different from other runs.

## APPENDIX G

Values of the kinetic model parameters from the parallel adsorption model, using linear regression analysis

The parameters  $k_1C$  and  $k_2C$  are determined by linear regression analysis of the experimental data fit to the kinetic model 2, suggested by McGuire et al. (1994b). The experimental data is divided into 2 regions, namely low contact time and high contact time. The low contact time region covers the adsorption time between 0 to 60 minutes. The high contact time region covers the adsorption time between 61 and 480 minutes. During the low contact time the adsorption rate is high and molecules occupy area on the contact surface quickly. During the high contact time the adsorption is slow and approximately a linear plot.

**Table G.1.** Values of the kinetic model parameters from the parallel adsorption model for each protein on hydrophilic surfaces, using linear regression analysis.

Protein	Run #	Date of Exp.	$k_1C$ ( $\times 10^4$ )	$k_2C$ ( $\times 10^4$ )	$k_2/k_1$
Wild Type	1	11/01/93	2.0483	1.8255	0.89
	2	12/12/93	1.7651	1.9597	1.11
	3	12/14/93	0.5586	1.4414	2.58
	4	12/30/93	1.3479	0.5460	0.41
M135	1	12/31/93	1.3753	0.6752	0.49
	2	01/14/94	0.7923	1.4728	1.89
	3	04/16/94	0.8037	1.1357	1.41
M135/147	1	01/03/94	1.9701	1.2938	0.66
	2	01/04/94	0.4929	1.9465	3.95
	3	01/05/94	0.8510	1.4924	1.75
	4	01/07/94	1.7816	1.4305	0.80

**Table G.2.** Values of the kinetic model parameters from the parallel adsorption model for each protein on hydrophobic surfaces, using linear regression analysis.

Protein	Run #	Date of Exp.	$k_1C$ ( $\times 10^4$ )	$k_2C$ ( $\times 10^4$ )	$k_2/k_1$
Wild Type	1	01/25/94	1.1112	1.6535	1.49
	2	02/01/94	0.2766	0.7694	2.78
	3	02/08/94	0.6696	1.8628	2.23
	4	02/13/94	0.5322	2.7810	5.23
M135	1	01/18/94	0.2958	2.2295	7.54
	2	01/20/94	0.7448	1.9219	2.58
	3	01/27/94	0.4810	1.2412	2.58
	4	02/12/94	0.6108	2.4120	3.95
M135/147	1	04/07/94	0.5771	1.8118	3.14
	2	06/28/94	0.0828	0.6243	7.54
	3	06/29/94	1.4847	1.1921	0.80

## APPENDIX H

### Raw data of all experiments

All raw data and associated information in this research are kept in diskettes with Ar. Joseph McGuire in Department of Bioresource Engineering, Gilmore Hall, Oregon State University, Corvallis, OR 97331.